

Study of EL and Transport Properties of Zn Metal Complex Based Materials for OLED Applications

A Thesis Submitted

In Partial Fulfilment of the Requirements

for the degree of

MASTER OF TECHNOLOGY

IN

MATERIALS SCIENCE AND ENGINEERING

BY

Deepa Rajwar

(Roll No: 60602006)



SCHOOL OF PHYSICS AND MATERIAL SCIENCE

THAPAR UNIVERSITY

PATIALA-147004, INDIA

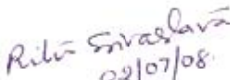
June 2008

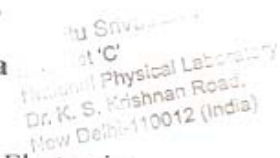
CERTIFICATE

This is to certify that the thesis entitled “**Study of EL and Transport Properties of Zn Metal Complex Based Materials for OLED Applications**” submitted by Miss Deepa Rajwar is in partial fulfillment for degree of Master of Technology in Materials Science and Engineering of this University. This work has been done under our supervision. The work presented in this thesis is original to the best of our knowledge and has not been submitted to any other degree of this or any other university.

The thesis work has been carried out from 02.01.2008 to 30.06.2008

Supervisors



02/07/08
Dr. Ritu Srivastava
Scientist
Centre for Organic Electronics
National Physical Laboratory, New Delhi

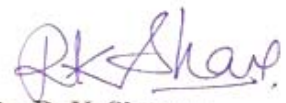

National Physical Laboratory
Dr. K. S. Krishnan Road,
New Delhi-110012 (India)



Dr. Dwijendra Pratap Singh
Lecturer
School of Physics and Materials Science
Thapar University, Patiala

Countersigned by:


Dr. O. P. Pandey
Prof. & Head
School of Physics and Materials Science
Thapar University, Patiala


Dr. R. K. Sharma
Dean, Academic Affairs
Thapar University, Patiala

ACKNOWLEDGEMENT

I express my deep sense of gratitude to Dr. M. N. Kamlasanan for providing me an opportunity to work in Centre for Organic Electronics, NPL. His astonishing language skills and his clear vision of scientific content help me in tremendous manner.

Words can hardly express my sense of gratitude to Dr. Ritu Srivastava for her invaluable supervision during the course of my thesis work. Dr. Srivastava was always available and helpful. Her great knowledge and wonderful attitude help in my training tremendously; her kindness, patience are much appreciable.

I want to express my deep sense of gratitude to my supervisor Dr. D. P. Singh. His wide knowledge and logical way of thinking have been of great value for me.

I express my gratitude to Dr. O. P Pandey, Head, School of Physics and Material Science, Thapar University Patiala for his invaluable support and encouragement.

I wish to express my sincere thanks to Dr. Vikram Kumar (Director NPL), for permitting and providing the facilities necessary for carrying out thesis work at NPL.

Dr. A. K. Gupta, Dr. S. S. Bawa, Dr. A. K. Aggarwal Head HRD group, NPL, for their support and encouragement during the course of thesis work. I am extremely thankful to Dr. Suresh Chand, Dr. S. K. Dhawan, for their invaluable help.

I also want to thanks Mr. Dharamveer Siani, from HRD group for his kind help.

I am deeply indebted to my teachers, Dr. K. K. Raina, Dr. N. K. Verma, Dr Kulvir Singh, Dr. Sunil Kumar, Dr. Manoj Kumar, Dr. S. Das, and Dr. S. D. Tiwari. Their ideals and concepts have had a remarkable influence on my understanding in the field of Material Science and Engineering.

I would like to give my special thanks to Miss Gayatri Chauhan, Mr. Virendra Kumar Rai,, Mr. Arunandan Kumar, Miss Manisha Bajpayi , Miss Priyanka Tyagi, Miss Rakhi, Miss Omvati members of Centre for Organic Electronics for their kind support in my work. Miss Gayatri and Mr. Arunandan helped me in all possible ways. Their timely discussions are very

timely discussions are very much appreciable. I also want to thanks my training mates and juniors Miss Namita Gandhi and Mr. Arjun Singh.

I want to express my heartfelt thanks to my most valuable friend Late Shri Manish Raj Arya. In my hard times, you pushed me always in the right direction. Only because of your inspiration I am going towards the successful completion of my M.Tech. Degree. I wish to express my warm and sincere thanks to all my friends (Specially, Mr. Alok Kumar, Miss Ashu, Miss Divya Rani, Mr. Narendra Kumar, Mr. Sandeep Kumar, Miss Suksham Charu, Miss Navreet, Miss Monika) who devoted their valuable time and helped me in all possible ways towards successful completion of this work.

I owe my most sincere gratitude to my parents, brothers whose honest support and obstinate love give me energy to complete this work successfully and gave me untiring help during my difficult moments. They have always wanted the best for me and I admire my parent's determination and sacrifice to put me through college.

Lastly I want to thanks Mr. Raju, and Mr. Hamant Kumar for their help in arranging laboratory materials during experiments. I will never forget Raju Bhaiya's nice tea.



DEEPA RAJWAR

ABSTRACT

Organic semiconductors have attracted lot of attention in academic and technological community due to its potential applications in organic light emitting diodes (OLEDs), organic photovoltaic cells etc. OLED is being considered as one of the most promising technology for flat-panel displays and in general lighting. The most important part of OLED devices is the electroluminescence layer, for which polymer and small molecular weight metal chelates can be used. The small molecule based metal chelates are the appropriate candidates as they are processed by conventional vacuum deposition techniques. Small molecule based Zn metal complexes can be used in OLED devices as electron and hole transport layer. It can also be used an emissive layer because of their wide spectral response in the visible region.

Two zinc complexes bis(8-hydroxy quinolate) zinc (Znq_2) and bis(2-methyl 8-hydroxy quinolate) zinc $Zn(mq)_2$ have been synthesized and characterized by different characterization techniques (FTIR, TGA, UV visible and Photoluminescence Spectroscopy). Both the photoluminescence and electroluminescence properties are extensively studied. The Photoluminescence properties of thin films of Znq_2 shows maximum absorption at 380 nm, extinction coefficient of $7.788 \times 10^3 \text{ moles}^{-1}\text{LCm}^{-1}$, photoluminescence peak at 542 nm and a quantum yield of 41 % and that of $Zn(mq)_2$ shows maximum absorption at 385 nm, an extinction coefficient of $1.869 \times 10^3 \text{ moles}^{-1}\text{LCm}^{-1}$ photoluminescence peak at 530 nm and a quantum yield of 21 %.

Organic light emitting diode have been fabricated with the structure ITO/ α -NPD(40 nm)/ Znq_2 (35 nm)/BCP(6 nm)/Alq₃(30 nm)/LiF(1 nm)/Al(100 nm) which shows a broad electroluminescence peak at 558 nm . The I-V characteristics of the device shows turn on voltage about 10.5 V and a maximum brightness 623 cd/m^2 at 18 V. Similarly an organic light emitting diode of $Zn(mq)_2$ as an emissive material with the structure ITO/ α -NPD(40 nm)/ $Zn(mq)_2$ (35 nm)/BCP(6 nm)/Alq₃(30 nm)/LiF(1 nm)/Al(100 nm) have been fabricated. An electroluminescence peak at 539 nm has been observed. The I-V characteristics of the device $Zn(mq)_2$ as an emissive material) shows turn on voltage about 4.5 V and a maximum brightness 752 cd/m^2 at 18 V.

Hole only devices of both the Zinc metal complexes [Znq_2 and $Zn(mq)_2$] have been fabricated. The injection limited current behavior has been observed for both the complexes. I-V characteristic of both the devices shows a temperature independent behaviour. Flower Nordiem model fits for both and the injection barrier height have been calculated for Znq_2 and $Zn(mq)_2$ device respectively.

CONTENTS

CHAPTER-1

INTRODUCTION

1.1 Historical Background	1
1.2 Limitations of Inorganic Light Emitting Diodes	1
1.3 Organic Light Emitting Diode an Introduction	2
1.3.1 Construction of an OLED	5
1.3.2 OLED Components	5
1.3.3 Working principle	6
1.3.4 Device Efficiency	7
1.3.5 Advantages	8
1.3.6 Applications of OLEDs	9
1.3.7 Challenges and Critical Issues	9
1.4 Electroluminescent materials used in OLED	10
1.4.1 Polymers	11
1.4.2 Small molecules	11
1.5 Metal complexes and there selection criteria	13
1.6 Deposition Techniques for OLED fabrication	15
1.7 Charge Injection and Transport Studies in Organic Semiconductors	17

CHAPTER-2

MOTIVATIONS AND SCOPE OF THE WORK

2.1 Motivation	20
2.2 Scope of the work	26

CHAPTER-3

EXPERIMENTAL

3.1 Synthesis	27
3.1.1 Synthesis of Bis(8-Hydroxyquinoate)(Zinc) Znq ₂	27
3.1.2 Synthesis of bis(2-methyl- 8-Hydroxyquinlate)(Zinc) Zn(mq) ₂	27
3.2 Material Characterization, device fabrication techniques	28

3.2.1 Materials characterization	28
3.2.1.1 UV-Visible Absorption Spectroscopy	28
3.2.1.2 Photo luminescent (PL) Spectroscopy	31
3.2.1.3 Fourier Transforms Infra-Red (FT-IR) Spectroscopy	32
3.2.1.4 Thermo Gravimetric Analysis	34
3.2.2 Device Fabrication Techniques	34
3.3 Device Fabrication	36
3.3.1 Znq ₂ and Znmq ₂ based Organic Light Emitting Device	36
3.3.2 Hole-only Devices Based on Znq ₂ and Zn(mq) ₂ materials for transport Studies	37
CHAPTER-4	
RESULTS AND DISSCUSSION	
4.1 Structural and thermal characterization	39
4.1.1 Structural and thermal characterization of Znq ₂	39
4.1.2 Structural and thermal characterization of Zn(mq) ₂	40
4.2 Optical characterization	42
4.2.1 Optical characterization of Znq ₂	42
4.2.2 Optical characterization of Zn(mq) ₂	43
4.3 Device characterization	44
4.3.1 Device characterization of Znq ₂	44
4.3.2 Device characterization of Zn(mq) ₂	47
4.4 Low Temperature I-V measurements and Transport Studies	50
4.4.1 Transport Studies of Znq ₂	50
4.4.2 Transport Studies of Zn(mq) ₂	52
CHAPTER-5	
CONCLUSION AND FUTURE SCOPE	
5.1 Conclusion	55
5.2 Future Scope	56
References	57

LIST OF FIGURES

Figure 1.1: Luminescent Aluminium chelates	3
Figure 1.2: Luminescent Beryllium chelates	4
Figure 1.3: Luminescent Boron chelates	4
Figure 1.4: Luminescent Zinc chelates	5
Figure 1.5: OLED components	6
Figure 1.6: Charge transport and light generation in OLED's	7
Figure 1.7 (a): Principle of Luminescent metal chelate	13
Figure 1.7(b): Luminescent chelate	13
Figure 1.8: Thermal vapour evaporation technique	16
Figure 1.9: Spin coating	17
Figure 3.1: Scheme- Synthesis of Znq_2	27
Figure 3.2: Scheme- Synthesis of $Zn(mq)_2$	28
Figure 3.3: Block diagram of UV-Vis spectrometer	29
Figure 3.4: Energy level diagram	30
Figure 3.5: Schematic diagram of luminescence experiment	32
Figure 3.6: Set-up of FT-IR (modle510p)	33
Figure 3.7: Device structure of OLED ($Znq_2/Zn(mq)_2$ as an emitter)	37
Figure 3.8: Hole-Only device	38
Figure 4.1: FTIR spectrum of Znq_2	39
Figure 4.2: Thermo Gravimetric Analysis (TGA) of Znq_2	40
Figure 4.3: FTIR spectrum of $Zn(mq)_2$	41
Figure 4.4: Thermo Gravimetric Analysis (TGA) of $Zn(mq)_2$	42
Figure 4.5: UV-Visible and Photoluminescence spectrum of Znq_2	43
Figure 4.6: UV-Visible and Photoluminescence spectrum of $Zn(mq)_2$	44
Figure 4.7: Photoluminescence and Electroluminescence spectra at different voltages	45
Figure 4.8: I-V-L characteristics of the device	46
Figure 4.9: J - L characteristics of the device	47
Figure 4.10: Photoluminescence and Electroluminescence spectra	48

at different voltages

Figure 4.11: I-V-L characteristics of the device	49
Figure 4.12: J-L characteristics of the device	49
Figure 4.13: Current -Voltage characteristics of the device showing temperature independent behaviour	51
Figure 4.14: The Fowler - Nordheim plot, $\ln(I/F^2)$ vs $1/F$, of Znq_2 device	52
Figure 4.15: Current -Voltage characteristics of the $Zn(mq)_2$ device showing temperature independent behaviour	53
Figure 4.16: The Fowler - Nordheim plot, $\ln(I/F^2)$ vs $1/F$, of $Zn(mq)_2$ device	54

LIST OF TABLES

Table (1)	Inorganic vs. Organic material	1
Table (2)	PL emission (nm) of different Zinc metal complexes	14
Table (3)	Summary	23

LIST OF PUBLICATIONS:

Conferences/symposia:

Presented a poster on “SYNTHESIS AND CHARACTERIZATION OF BIS (2-METHYL 8-HYDROXY QUINOLINATE) ZINC $Zn(mq)_2$ FOR ORGANIC LIGHT EMITTING DIODES ” in **Third International Conference on Luminescence and its Applications(ICLA-2008)** held at National Physical Laboratory Delhi on 13-16 Feb 2008.

International Journal

Communicated a paper on “SYNTHESIS AND CHARACTERIZATION OF BIS (2-METHYL 8-HYDROXY QUINOLINATE) ZINC $Zn(mq)_2$ FOR ORGANIC LIGHT EMITTING DIODES ” in *Materials Chemistry and Physics* (communicated).

CHAPTER- 1
INTRODUCTION

1.1 Historical Background

Several factors are driving the recent development of light emitting devices (LEDs). The most important ones are brightness, available efficiency, flexibility, rugged construction and low applied voltages. These are contributing to growth in markets such as traffic lights, automotive brake signals, instrument and video displays and the many uses of the new white LED-based products. A new development [1, 2] is directed to various materials used for high brightness based on AlGaAs (red), AlInGaP (yellow-green to red) and InGaN (blue, green and white) devices. Due to their epitaxial complexity the development of LEDs depends on epitaxial growth advances in compound semiconductor technologies, mainly molecular beam epitaxy (MBE) and metal-organic vapor phase epitaxy (MO VPE). So, that the main engineering challenge is now the extraction or the ability to get all the light out of the chip to where it is needed.

Many of today's solid-state inorganic microelectronic devices [3, 4] are reaching their theoretical limits. The increasing cost of smaller component fabrication combined with the increased power dissipation of higher component density devices beckons the need for an alternative. Although this fact is best illustrated in the realm of microprocessors, its effects are still felt in the area of active displays – one in which organic light-emitting diodes (OLEDs) look to supplant the present standard of liquid crystal displays (LCDs) and solid-state light-emitting diodes (LEDs) [5].

1.2 Limitations of Inorganic Light Emitting Diodes

- Single Crystalline- limitation of area
- Epitaxial films - lattice matching problems
- Large processing and material cost
- Non flexible
- High refractive index-difficult to extract light out of the devices

Following table (1) shows a brief comparison between Inorganic and Organic materials used for LED applications.

Table (1): Inorganic vs. Organic material

Characteristic	Organic	Inorganic
Structure (morphology)	Amorphous	Single crystalline
Charge Carrier Properties	Molecular	Lattice
Mobility (cm ² /Vs)	10 ⁻³ to 10 ⁻⁵	1 to 1500
Processing	Low temperature	High temperature
Synthetic flexibility	High	Low
Stability	Currently an issue	Very good
Construction	<div style="display: flex; justify-content: space-around;"> <div style="text-align: center;"> <p><u>Organic LED</u></p> </div> <div style="text-align: center;"> <p><u>Inorganic LED</u></p> </div> </div>	

1.3 Organic Light Emitting Diode an Introduction

Organic electroluminescent (EL) materials and devices have attracted much attention and interest in recent years because of their potential application in flat panel displays [5-8]. These materials for EL devices can be classified into three categories according to their molecular structure: 1) organic dyes (no metal element), 2) chelate metal complexes, and 3) polymers [7]. The metal complexes are especially important

because of the simplicity in synthesis procedures, ease of fabrication, high thermal stability and the wide spectral response [8, 9]. There are many factors affecting the photoluminescence efficiency of these metal complexes. The most common and important factor is the thermal vibration of the chromophore, which provides a path for the loss of energy via a radiationless pathway. One can reduce the loss of energy via thermal vibration by increasing the rigidity of the chromophore. For coordination compounds, this reduction can be achieved by chelating the appropriate chromophore to a suitable metal ion, which reduces the degree of freedom of thermal vibrations of the chromophore, thus increasing its emission efficiency [10]. Further, metal chelates can be prepared very pure and can have high luminescence quantum yields and high stabilities at high operating voltages. The choice of metal ions for EL chelates is limited to those metals which do not exhibit d-d transitions that may interfere with the luminescence of the ligand. Therefore, aluminium (III) (Figure 1.1), boron (III) (Figure 1.2), beryllium (II) (Figure 1.3) and zinc (II) (Figure 1.4) are ideal. Since beryllium (II), boron (III) and aluminium (III) has no 'd' electron and zinc (II) has a closed shell of d electrons. The metal ions only have a structural purpose by stabilizing a luminescent ligand [10]. These metal complexes can be used both as an electron transport layer, and as an emissive layer. Zinc metal complexes have a wide range of spectrum in the visible region [7]. Extensive research work is going on in various laboratories to synthesize new zinc complexes containing new ligands to produce a number of novel luminescent zinc complexes as emitters [11-16] and electron transporters [17-19] in OLED research.

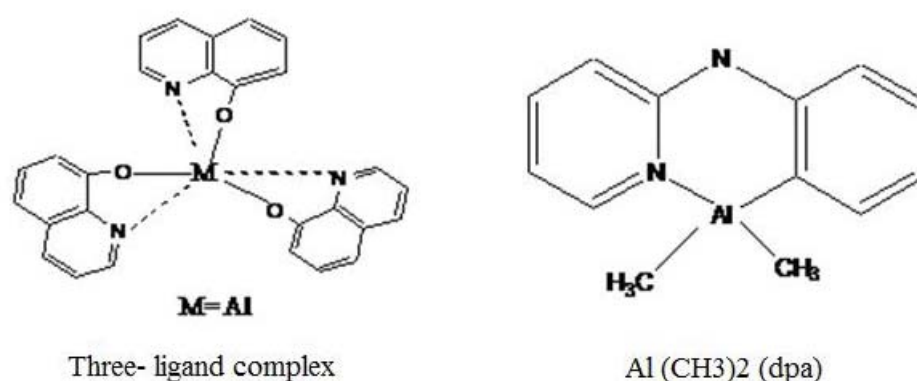
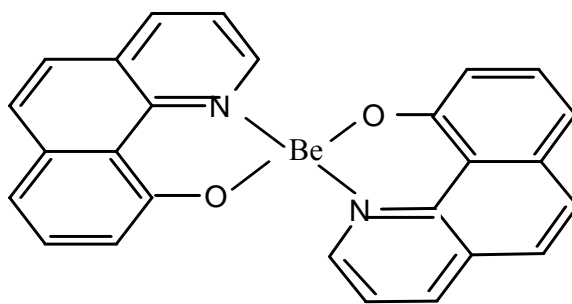


Figure 1.1: Luminescent Aluminium chelates.



BeBq_2

Figure 1.2: Luminescent Beryllium chelates.

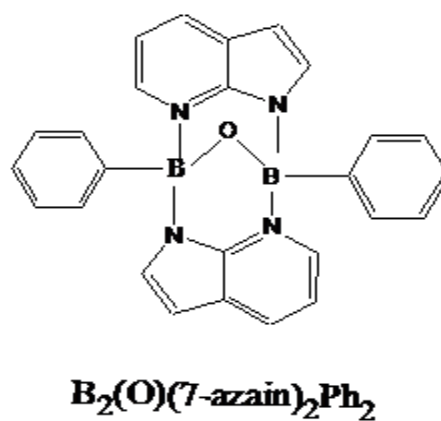
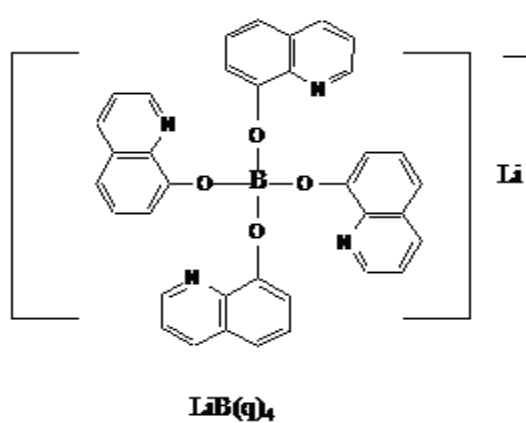
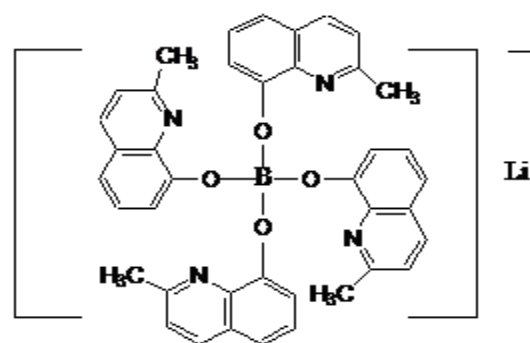
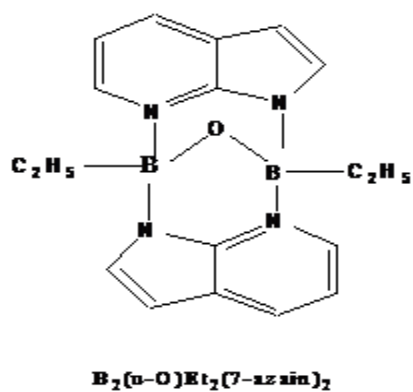


Figure 1.3: Luminescent Boron chelates.

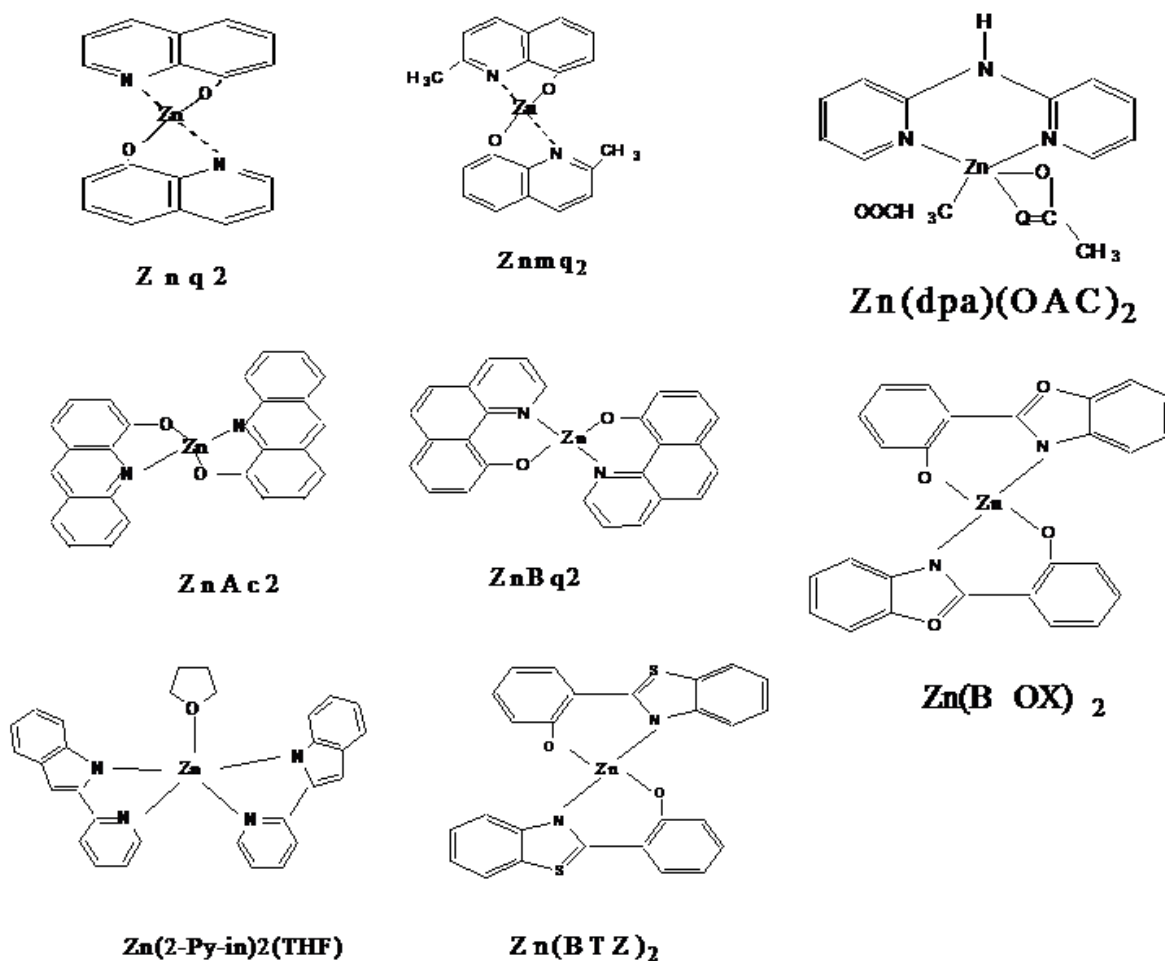


Figure 1.4: Luminescent Zinc chelates.

1.3.1 Construction of an OLED

A typical OLED consists of two organic layers (electron and hole transport layers), embedded between two electrodes. The top electrode is usually a metallic mirror with high reflectivity and the bottom electrode a transparent ITO layer on the top of the glass substrate (Figure 1.5).

1.3.2 OLED Components

Like an LED, an OLED is a solid-state semiconductor device that is 100 to 500 nanometres thick or about 200 times smaller than a human hair. OLEDs can have either two layers or three layers [20] of organic material; in the latter design, the third layer helps in transportation of electrons from the cathode to the emissive layer.

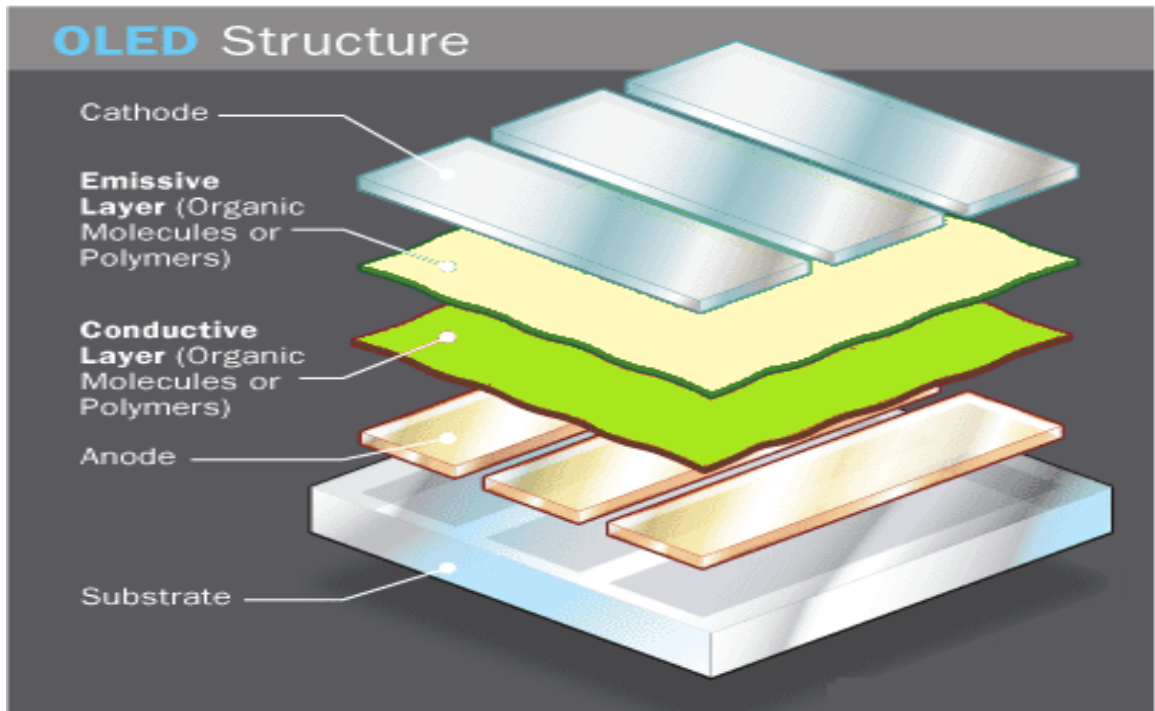


Figure 1.5: OLED components.

1.3.3 Working principle

When electricity is applied to OLED, charge carriers (holes and electrons) are injected from the electrodes into the organic thin films. They migrate through the device under the influence of an electrical field. The charge carriers then recombine, forming excitons. In the past, conventional wisdom suggested that only about 25 % of these excitons could generate light, with the remaining 75 % lost as heat. This was known as fluorescent emission. Through a breakthrough by academic partners at Princeton University and the University of Southern California, however, 100 % of the excitons can be converted into light using a process known as electro phosphorescence, now commonly referred to as phosphorescence. Thus, the efficiency of a phosphorescent OLED is up to four times higher than that of a conventional fluorescent OLED.

When a voltage is applied to the electrodes the charges start moving in the device under the influence of the electric field. Electrons leave the cathode and holes move from the anode in opposite direction. The recombination of this charges leads to the creation of a photon with a frequency given by the energy gap ($E = h\nu$) between the LUMO and HOMO levels of the emitting molecules (**Figure 1.6**). Therefore, the electrical power applied to the electrodes is transformed into light [21].

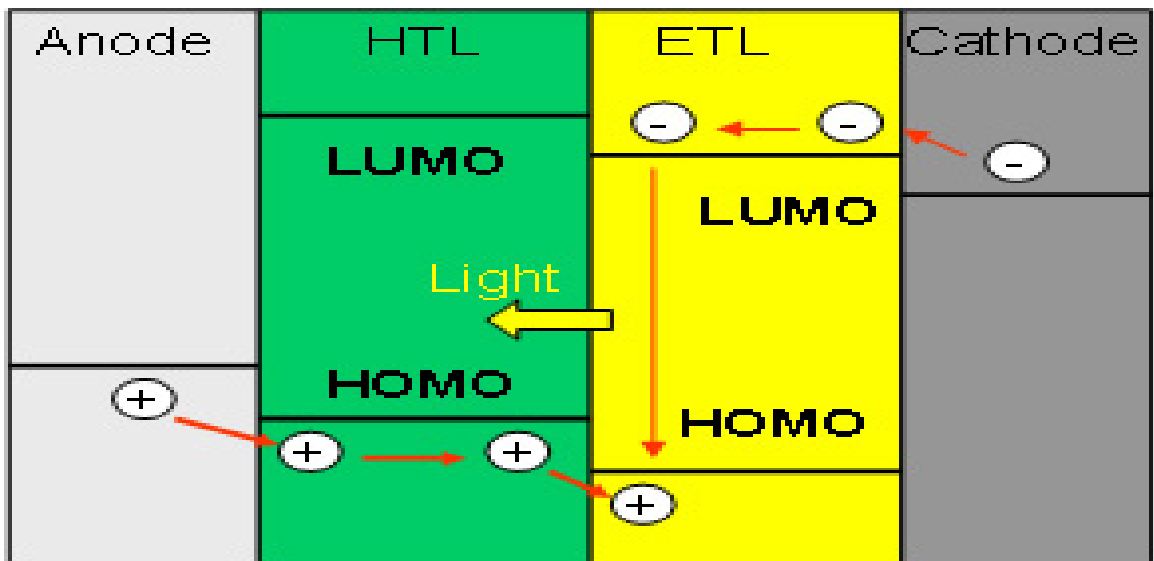


Figure 1.6: Charge transport and light generation in OLED's.

1.3.4 Device Efficiency

The efficiency [22] of OLEDs can be characterized by its

- a. Quantum efficiency,
- b. Power efficiency (lm/W),
- c. Luminous efficiency (cd/A), sometimes called luminous yield.

a. Quantum efficiency

The device quantum efficiency η_q has two parts: internal and external:

(1) Internal quantum efficiency η_{int} or I_{QE} is the number of photons generated inside the device per number of injected hole – electron pairs. A large fraction of generated photons stays trapped and absorbed inside the device.

(2) External quantum efficiency η_{ext} or E_{QE} , is the number of photons released from the device per number of injected hole – electron pairs.

b. Power efficiency (lm/W)

Luminous (Power) efficiency η_p is the ratio of the lumen output to the input electrical watts (lm/W).

c. Luminous efficiency (Current efficiency) (cd/A)

Luminous efficacy η_v represents the ratio of the lumen output to the optical watts (radiative power). The luminous efficiency and luminous efficacy of a device account for a spectral sensitivity of a human eye. Therefore, two devices with similar quantum efficiencies can have different luminous performance, depending on the spectrum of the emitted light. In the process of converting electrical power into optical power, losses are incurred due to non-radiative processes (thermal relaxation of excitons, internal reflection and absorption of photons).

1.3.5 Advantages

Robust Design - OLED's are tough enough to use in portable devices such as cellular phones, digital video cameras, DVD players, car audio equipment and PDA's.

Viewing Angles – Can be viewed up to 160 degrees, OLED screens provide a clear and distinct image, even in bright light.

High Resolution – High information applications including videos and graphics, active-matrix OLED provides the solution. Each pixel can be turned on or off independently to create multiple colors in a fluid and smooth edged display.

Electronic Paper – OLED's are paper-thin. Due to the exclusion of certain hardware goods that normal LCD's require, OLED's are as thin as a dime.

Production Advantages – Up to 20 % to 50 % cheaper than LCD processes. Plastics will make the OLED tougher and more rugged. The future quite possibly could consist of these OLED's being produced like newspapers, rather than computer "chips".

Video Capabilities – They hold the ability to handle streamlined video, which could revolutionize the PDA and cellular phone market.

Hardware Content – Lighter and faster than LCD's. Can be produced out of plastic and is bendable. Also, OLED's do not need lamps, polarizers, or diffusers.

Power Usage – Takes less power to run (2 to 10 volts).

1.3.6 Applications of OLEDs

Monochrome applications

- Small monochrome displays for hand held electronic devices (cell phones, PDAs, digital cameras, GPS devices etc.) already in the marketplace.
- Niche applications such as head-mounted displays.

Two or multicolour applications

- Car electronics (radios, GPS displays, maps, warning lights, etc.).
- Instrument electronics, heads-up instrumentation for aircraft and automobiles.
- Rugged PDAs, wrist-mounted, etc. Some are already on the market.

Full colour application

- LCD backlights (white light)
- Small full colour displays. To be introduced within a year.
- Full colour, high-resolution, personal communicators

Large displays

- Wall-hanging TV monitors
- Large screen computer monitors

Applications Convertible to OLEDs

General White applications (to replace incandescent/halogen) and General White applications (to replace fluorescent)

- Lighting panels for illumination of residential and commercial buildings.
- Lighting panels for advertising boards, large signs, etc.
- Ultra-lightweight, wall-size television monitors.
- Office windows, walls and partitions that double as computer screens.
- Colour-changing lighting panels and light walls for home and office, etc.

1.3.7 Challenges and Critical Issues

Even though remarkable progress has been made, OLEDs still face great challenges before commercialization as white-light sources can be even considered. OLEDs have

already achieved power conversion efficiencies close to those needed for energy efficient operation, but only for the green and red light, and with insufficient luminance. Other colors are still far beyond. The peak brightness can be greater than several hundreds of thousands cd/m^2 , but these devices degrade very quickly. The operating voltages can be as low as the desired 2.6 V- 4 V but the luminance are still too low under those voltages. For white light and the desired luminance, the passing electric currents are still too high, and the power conversion efficiencies are low. The useful lifetime of white-light emitting devices with the desired luminance needs to be increased by more than one order of magnitude. The surface area of the largest devices made to date is only of the order of a couple of square inches, while the illumination panels will have to cover several square feet. The uniformity of these devices is far worse than desired, etc.

The technological issues facing [23] OLEDs can be summarized into the two main categories:

- Operational life and Power conversion efficiency of OLEDs.
- Cost of manufacturing, the lack of infrastructure.

Specifically, to effectively compete with, and eventually displace fluorescent lighting, these challenges are:

- (1) Efficacy improvement to obtain 120 lm/W for white light for a 1000 lm white source and useful life 20,000 hrs.
- (2) Cost of manufacturing so as to be lower than for traditional light sources.
- (3) Development of new infrastructure including powering of high current-low voltage distributed sources, new industries and technologies that are enabled by attributes of OLED.

1.4 Electroluminescent materials used in OLED

Materials used for the fabrication of organic light emitting diodes are of organic origin and semi conducting in nature, during the fabrication of the OLED it's important to select an appropriate electroluminescent material for proper function and best performance.

The materials for OLED is broadly divided into two divisions

a. Polymers

b. Small Molecules

1.4.1 Polymers

Besides their roles as inert binders, polymers have been used [24] in OLEDs as electroluminescent materials since the late 1980s, when emission was observed in poly (1, 4-phenylene vinylene). The major advantage of using polymers [25] over small organic molecules is that polymers can be solution processed. The simplicity of solution processing equates to a low manufacturing cost, which can lead to techniques known as roll-to-roll processing and ink-jet printing. Roll-to-roll processing is a technique in which a polymer solution is sprayed onto a large flexible substrate which already contains the anode. After deposition of the cathode, the substrate can then be cut into smaller sections depending on the final application of the OLED. Ink-jet printing is a high-resolution patterning of red, green, and blue light-emitting polymers using the same technology found in an ink-jet printer. Based on a drop diameter of 20 μm and a 100 nm thick layer, ink-jet printing can use polymer solutions with concentrations as low as 1 %. Polymers in OLEDs are used as emissive as well as hole transport layer and electron transport layer.

1.4.2 Small molecules

Small molecule materials [7, 26] for OLEDs are generally low molecular weight organic molecules or complexes of organic molecules. These are generally coated onto the suitable substrates by the process of vacuum deposition to yield thin amorphous films. However, they can be blended into a polymer matrix or grafted into a polymer backbone so that they can be applied easily by spin coating. The requirements for an organic small molecule or complex to be used in the form of an emission layer in the device are that it should be thermally stable to enable vacuum deposition, highly luminescent in the solid-state and should be thin-film forming. Also, it should be able to transport electrons with the desired efficiency. Although wide ranges of metal chelates are highly luminescent in solution, few are able to satisfy all the above criteria. The discovery of the highly successful tris (8-hydroxyquinoline) aluminum[6,8] as an efficient electron transport and electroluminescent material lead to further research and development in this field, and now there are a wide variety of small molecule emitters with varied emission

wavelengths to choose from. Because light emission from the Alq₃ complexes originates from the electronic transitions located on the quinolinolate ligands (ligand-centered excited states). The HOMOs are located on the phenoxide side of the ligand, while the LUMOs are located on the pyridine ring. Thus the attachment of electron-donating substituents to the phenolate ring results in a red-shifted emission, while the attachment of electron-donating substituents to the pyridine ring results in a blue-shifted emission from the complex. Additionally, the nature of the metal ion has been shown to have a profound effect on the quinolinolate photoluminescence and electroluminescence. With increased covalent nature of the metal-ligand bonding (primarily metal-nitrogen bond), the emission is red-shifted, while the more ionic bond in strongly electropositive metal ions results in a blue shift.

Progress of Small Organic Molecular Luminescent Materials

Small organic molecules and some coordination complexes are considered promising luminescent materials because they have obvious advantages over polymers. First they can be purified easily so that they may have high fluorescence efficiency. Second they can be fabricated into thin films by sublimation. The most important advantage is that small molecular materials have a wider selection of emission colour than polymers, especially in the blue region, since the structure of a small molecule can be modified readily to achieve the desired energy band gap.

Principles of Luminescent Metal chelate

The requirement for a material to be a good electro luminescent material is that it must be a good photo luminescent material. A good photo luminescent compound should also have high thermal and air stability, high volatility and high emission efficiency. A promising strategy for the production of useful luminescent materials involves the synthesis of metal chelates. The metal typically acts as a tether, associating with one or more ligands with luminescent properties. Luminescent metal chelates [10] contain one or more organic chromophores and supporting Metal Substituent legands attached to the metal centre (or a main group element such as boron) via a donor acceptor bond or a covalent bond. Because metal chelate (**Figure 1.7(a)**) compounds are supporting part chromophore(**Figure 1.7(b)**) small molecules, they can be sublimed readily; Luminescent chelate when appropriate ligands are present.

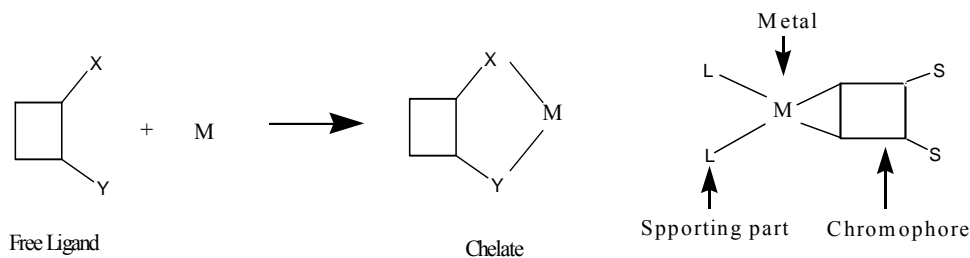


Figure 1.7(a)

Figure 1.7(b)

**Figure 1.7 (a): Principle of Luminescent metal chelate Figure 1.7(b):
Luminescent chelate**

1.5 Metal complexes and there selection criteria

We have concentrated on the studies of small molecules, because they are easy to handle in conventional vacuum deposition equipment. There are a large variety of small fluorescent molecules but not so many molecules that can make uniform thin films in vacuum vapour deposition. If a small molecule can be sublimed in vacuum successfully, it often forms a polycrystalline film with many pinholes, which leads to device failure. Even when a uniform thin film is obtained, carrier transport ability and fluorescent yield of the film are the next problems. Knowing the energy bands of the HOMO and LUMO levels for a compound is also important in fabricating an organic EL cell.

To summarize, the following properties are strongly required or indispensable for the EL materials: (1) form a uniform thin film; (2) carrier (hole/electron) transport ability; (3) high fluorescent yield; (4) stable to heat (have a high glass-transition temperature); (5) suitable HOMO/LUMO levels for the carrier injections [27].

There are many factors affecting the emission efficiency of photoluminescence.

- The most common and important factor is the thermal vibration of the chromophore, which provides a path for the loss of energy via a radiationless pathway. One can reduce the loss of energy via thermal vibration by increasing the rigidity of the chromophore. For coordination compounds, this reduction can be achieved by chelating the appropriate chromophore to a

suitable metal ion, which reduces the degree of freedom of the thermal vibrations of the chromophore, thus increasing its emission efficiency.

- Compared with polymers, another advantage of metal chelates is that they can be prepared very pure. Therefore, they may have high luminescence quantum yields and high stabilities at high operating voltages.
- The choice of metal ions for EL chelates is limited to those metals which do not exhibit d-d transitions that may interfere with the luminescence of the ligand. Therefore, aluminium (III), boron (III), beryllium (II) and zinc (II) are ideal. Since beryllium (II), boron (III) and aluminium (III) has no d electron and zinc(II) has a closed shell of d electrons. The metal ions only serve a structural purpose by stabilizing a luminescent ligand.
- Zinc metal complexes can be used both as an electron transport layer, hole transport layer or as an emissive layer.
- Zinc metal complexes have a wide range of spectrum in the visible region [8, 11].

Photoluminescence emission (nm) of Zinc metal complexes can be summarized in the following **table (2)**.

Table (2): PL emission (nm) of different Zinc metal complexes

Compounds	PL Emission (nm)	
	Solution (in MeOH)	Solid
Znq ₂	-	535,567
ZnBq ₂	-	572
Zn(Ac) ₂	-	647
Zn(BTZ) ₂	-	486,524
Zn(BOX) ₂	-	478
Zn(dpa)(OAC) ₂	359	378
Zn(dpa)Cl ₂	360	378
Zn(dpa)(CN) ₂	359	363,418
Zn(dpa)(4-MeC ₆ H ₄ S) ₂	354	481

$[\text{Zn}(\text{dpa})_2][\text{CF}_3\text{SO}_3]_2$	360	373
$\text{Zn}(\text{tdpa})(\text{OAC})_2$	394	411
$\text{Zn}(\text{tdpa})\text{Cl}_2$	392	403
$[\text{Zn}(\text{tdpa})][\text{CF}_3\text{SO}_3]_2$	390	398

1.6 Deposition Techniques for OLED fabrication

Deposition techniques for the Organic materials can be classified in the following two broad categories.

A) Evaporation (Suitable for small molecules)

Evaporation techniques which is suitable for small molecules can be of following three types: Sputtering,

E-beam evaporation,

Vapour deposition

Electron -beam evaporation and sputtering are for high temperature material, (both available in clean room). Sputtering is especially useful for large substrates (Used for ITO). These methods can damage the organic layers since organic material have low glass transition temperatures. Vacuum evaporation (**Figure 1.8**) by direct heating is the most appropriate for organic materials. The pressure needed to deposit organic devices is about 10^{-5} - 10^{-6} torr. Deposition rate for organics is about 1-10 Å/s. Deposition Temperature depends on vacuum quality and material. Substrates should be kept at low temperature during deposition. Deposition rate is controlled by crystal monitor.

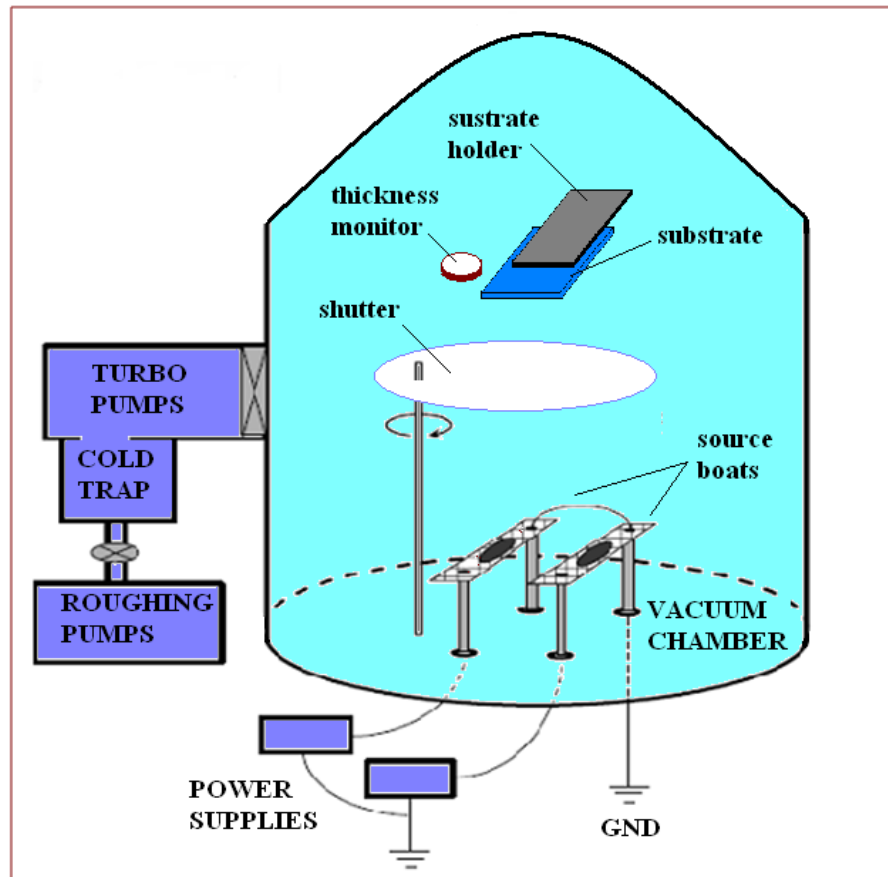


Figure 1.8: Thermal vapour evaporation technique

B) Wet processing (Suitable for polymers)

Wet processing which is suitable for polymers can be of two types: Spin coating, Inkjet printing. In the Spin Coating (**Figure 1.9**) process for polymer film deposition polymer solution is dropped on the rotating substrate. By centrifugal force, solution spreads on the substrate. Thin film properties depend on rotation speed curve, solution, temperature, vapour pressure of material. With inkjet technology, OLEDs are sprayed onto substrates just like inks are sprayed onto paper during printing. Inkjet technology greatly reduces the cost of OLED manufacturing and allows OLEDs to be printed onto very large films for large displays like 80-inch TV screens or electronic billboards.

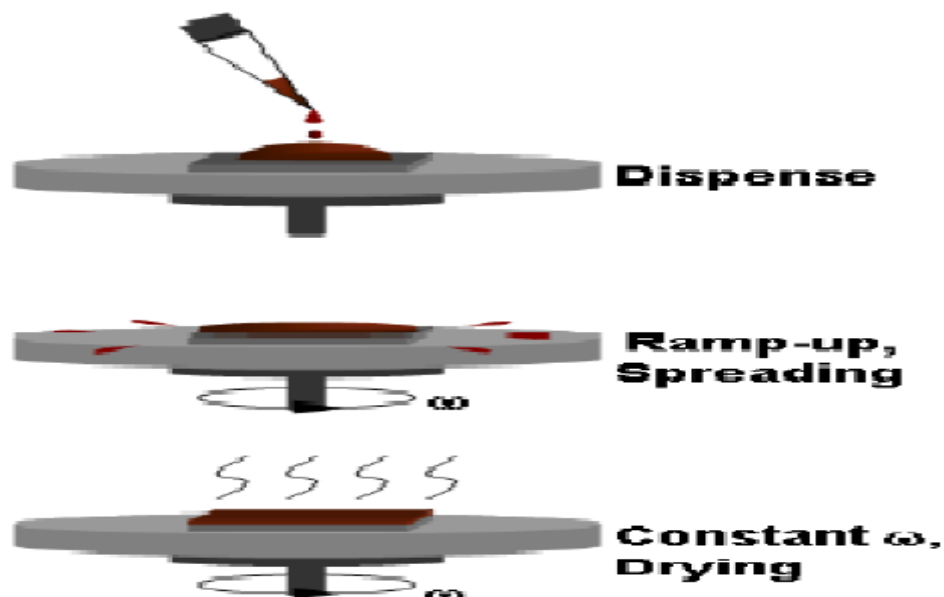


Figure 1.9: Spin coating

1.7 Charge Injection and Transport Studies in Organic Semiconductors

Light emission from an OLED occurs due to a recombination of injected electrons and holes in the molecules. Hence, an injection mechanism, a transport mechanism, and a recombination process are important in organic light-emitting diodes. In organic light-emitting diodes (OLEDs), organic materials' low carrier mobilities are thought to lead to the fact that the conduction mechanism in OLEDs corresponds to the space charge-limited current (SCLC) model. In polymer light-emitting diodes (PLEDs), the SCLC model is easily accepted because their layer structure is simpler than those of low molecular LEDs. Depending on the magnitude of the energy barrier Δ ($\Delta_h = I - \varphi_{\text{anode}}$ for holes and $\Delta_e = \varphi_{\text{cathode}} - A$ for electrons, where φ is the work function of the contact material and I and A are the ionization energy and electron affinity of the organic dielectric, respectively.), the current flowing through an OLED can either be space-charge limited (SCL) [28] i.e., transport limited, or injection limited.

The SCLC model ought to essentially be applied to unipolar conduction. When voltage is applied to an insulator (organic material) interposed by two electrodes and the charged carriers injected from an electrode are not neutralized by the counter

charged carriers injected from the counter electrode, the injected charged carriers form the space charge around the electrode. This space charge modifies the electric field between both electrodes in the case of low mobility. The homo space charge accumulated in front of an electrode reduces the electric field on the electrode. Therefore, the carrier injection after forming the space charge strongly depends on the modified electric field due to the space charge. A necessary condition for SCL conduction is that one of the contacts supply more charge carriers per unit time than can be transported through the organic dielectric. A contact that behaves in this way is called an ohmic contact. At an ohmic contact the electric field F vanishes owing to screening by the space charge associated with unipolar current flow. This requires an injection barrier [29] small enough to guarantee efficient injection without the assistance of an external electric field. The SCL current (SCLC) is the maximum unipolar current a sample can sustain at a given electric field unless the exit contact is able to inject opposite charge carriers sufficient to compensate for the internal space charge. In the absence of traps [30, 31] the SCLC obeys Child's law

$$j = \frac{9}{8} \epsilon \epsilon_0 \mu \frac{F^2}{L}$$

Where, ϵ is the relative dielectric constant, ϵ_0 the permittivity of vacuum, μ the charge-carrier mobility, and L the sample thickness.

For the OLEDs in which current is strongly controlled by injected carrier density (Science organic materials have low carrier concentration), some researchers analyzed the current of OLED as Schottky current model controlled by hole or electron injection. However, values of physical parameters, such as the dielectric constant and the barrier height of carrier injection, determined from the approximate I–V curve, differ greatly from those estimated direct measurements. Although some interpretations for the conflict are suggested, they are thought to be inconsistent with physical phenomena [32]. Injection-limited conduction is commonly described either by the Fowler-Nordheim (FN) model [33] for tunnelling injection or by the Richardson-Schottky (RS) model [34] for thermionic emission. The FN model ignores image-charge effects and considers the tunnelling of electrons from the contact

through a triangular barrier into unbound continuum states. It predicts a $j(F)$ characteristic, which is insensitive to temperature,

$$j_{FN} = BF^2 \exp\left[-\frac{b}{F}\right]$$

$$\text{Where } B = \frac{e^3}{8\pi h \Delta}, \quad \text{and} \quad b = \left[\frac{8\pi(2m^*)^{1/2}\Delta^{3/2}}{3he}\right]$$

Here e is the elementary charge, h the Planck constant, and m^* the effective mass of the carrier inside the dielectric.

The RS model assumes that an electron from the contact can be injected once it has acquired a thermal energy sufficient to cross the potential maximum resulting from the superposition of the external and the image-charge potential. Tunnelling through the barrier is ignored. The $j(F)$ characteristic is given by

$$j_{RS} = A^*T^2 \exp\left[-\frac{\Delta - \left(\frac{e^3}{4\pi\epsilon\epsilon_0}\right)^{1/2} F^{1/2}}{kT}\right]$$

where A^* is the Richardson constant, T the temperature, and k the Boltzmann constant.

CHAPTER-2

MOTIVATIONS AND SCOPE OF THE

THESIS

2.1 Motivations

For the first time in the year 1987 **C.W Tang and S.A VanSlyke** [6] constructed electroluminescent device using organic materials as the emitting elements. It has been found that the Electron-hole recombination and green electroluminescent emission are confined near the organic interface region. High external quantum efficiency (1 % photon/electron), luminous efficiency (1.5 lm/W), and brightness ($>1000 \text{ cd/m}^2$) has been achieved at a driving voltage below 10 V.

There is another work reported by **Yuji Hamada** [7] in 1997 in which several chelate metal complexes have been developed. RGB (red, green, and blue) emission has been achieved using only chelate metal complexes, after successfully obtaining high-luminance **blue-emitting materials, such as azomethine-zinc complex**. This shows that the chelate metal complexes can be applied to full-color flat displays as an emitting material. Bis (10-hydroxybenzo quinolinato) beryllium (BeBq_2) has been reported as an electron transport layer in OLED devices, with a lifetime (initial luminance: 500 cd/m^2) of more than 3500 h, which is a practical level.

Yoshiharu Sato, Shoko Ichinosawa et al [35] in the year 1998 reported that the degradation of the organic electroluminescent (EL) device is closely related to the physical and chemical stability of the organic thin films. They described three important aspects as:

- 1) An effect of glass transition temperature of hole transport materials on thermal stability of the device;
- 2) A role of interface layers at both the anode and cathode; and
- 3) An improvement of operation stability by doping technology.

Considering the above points, an organic EL device has been fabricated with a good operation performance: lifetime of longer than 3000 h at an initial luminance of 500 cd/m^2 .

A better performance has been observed by **S. E. Shaheen, G. E. Jabbour, et al** [36] using a triphenyldiamine side-group polymers as hole transport layers in multilayer organic light-emitting diodes using 8-hydroxyquinoline aluminum (Alq_3) as an emission layer.

The comparative study of electroluminescent properties of Tris (8-hydroxyquinoline) gallium Gaq_3 and 8-hydroxyquinoline zinc (Znq_2) has been investigated by **Yong Qiu,**

Wenhua Hu et al [37] in the year 2000. It has been reported that the solid film of Gaq₃ could yield a very strong photoluminescence (PL) and an EL device with Znq₂ could harvest a higher brightness even than Alq₃.

In the same year 2000 **Yoshitaka Nishio, Yuji Hamada et al [38]** reported the studies of small molecules which can form thin films on thermal vapour deposition. Following properties has been reported for the EL materials:

- (1) Form a uniform thin film
- (2) Carrier (hole/electron) transport ability
- (3) High fluorescent yield
- (4) Stable to heat (have a high glass-transition temperature)
- (5) Suitable HOMO/LUMO levels for the carrier injections

Degradation mechanisms in small molecule-based organic light-emitting devices (OLEDs) have been reviewed in the year 2002 by **Zoran D. Popovic and Hany Aziz [39]**.

In the year 2004 the electrical and optical properties of the NiO films deposited under various conditions has been first characterized by **I-Min Chan and Franklin C. Hong et al [40]**. It has been suggested that the NiO/ITO anode is an excellent choice to enhance the hole injection in OLED devices.

Again in the same year it has been reported by **N. N. Dinh, D. V. Thanh et al [41]** that the enhancement in both the onset electric field (onset voltage) and the reverse current are due to lowering the workfunction of Al/Alq₃ by the application of the super-thin LiF layer. These enable electrons better inject into the emissive Alq₃ material, consequently one can have higher possibility of emissive recombination of excitons in the devices.

In the year 2005 **Naiying Du, Qunbo Mei et al [19]** reported that the electron-donating substituent increased the solubility of the corresponding metal quinolate complexes in nonpolar solvents and caused a red-shift in the emission wavelength. The end groups of two compounds facilitated polymerization to form the metalloquinolate-containing polymers.

An azomethin-zinc complex, bis[salicylidene(4-dimethylamino)aniline]zinc(II) (Zn(sada)₂) has been synthesized and structurally characterized by **Junfeng Xie, Juan Qiao, et al [42]**. It has been found that compared

with the typical bilayer device of N,N'-diphenyl-N,N'-bis(1-naphthyl)-benzidine (NPB)/tris-(8-hydroxyquinoline)aluminum (Alq₃), the device with Zn(sada)₂ as the electron transporting layer exhibited a much lower turn-on voltage of 2.5 V (it is usually 3.5 V for an NPB/Alq₃ device).

In the recent year more work has been done on electroluminescent small molecules based on zinc metal complexes.

In 2006 new electroluminescence materials, including [2-(2-hydroxyphenyl) benzoxazole] (Zn(HPB)₂) and [(1,10-phenanthroline)(8-hydroxyquinoline)] Zn(phen)q has been synthesised by **Yoon-Ki Jang, Dong-Eun Kim [17]**. The photoluminescence (PL) spectra of Zn(HPB)₂ and Zn(phen)q has been observed to be blue and yellowish green, respectively.

In the same year zinc complexes (Zn(HPB)₂ and Zn(HPB)q) has been synthesized by **Kim, Won Sam; You, Jung Min; et al [43]**. It has been reported that the ITO/NPB (40 nm)/Alq₃ (60 nm)/Zn(HPB)₂ (5 nm)/LiF/Al device showed increased luminance of $L = 17000 \text{ cd/m}^2$ compared to $L = 12000 \text{ cd/m}^2$ for similar device fabricated without the hole-blocking layer.

Again in the same year **Christopher Williams et al [44]** reported High performance organic light-emitting diodes (OLEDs) implemented on transparent and conductive single-wall carbon nanotube sheets.

Enhanced photoluminescence intensity has been observed in the same year for the samples annealed in oxygen near 100 °C by **Vivek Kumar Shukla, Satyendra Kumar et al [45]**. Sudden change in roughness which may be as a consequence of change in surface morphology due to phase change and fraction of new phase is estimated by phase images taken by Atomic Force Microscopy (AFM) has been reported. The enhanced photoluminescence has been understood in terms of formation of a new phase.

The electroluminescence devices with the ZnL (where L is the ligand) complex as the emitting layer has been constructed, by **Tianzhi Yu et al [46]**, in the year 2007 which exhibited blue emission with a peak at 455 nm and the maximum brightness of 650 cd m^{-2} .

Table (3): Summary

Author	Work	Result
C.W Tang and S.A VanSlyke (1987)	Constructed electroluminescent device (Alq_3 based) using organic materials as the emitting elements.	High external quantum efficiency (1% photon/electron), luminous efficiency (1.5 lm/W), and brightness ($>1000 \text{ cd/m}^2$) has been achieved at a driving voltage below 10 V.
Yuji Hamada (1997)	Developed several chelate metal zinc complexes. RGB (red, green, and blue) emission has been achieved.	The chelate metal complexes can be applied to full-color flat displays as an emitting material.
Yoshiharu Sato, Shoko Ichinosawa et al (1998)	They reported that the degradation of the organic electroluminescent (EL) device is closely related to the physical and chemical stability of the organic thin films.	An organic EL device has been fabricated with a good operation performance: lifetime of longer than 3000 h at an initial luminance of 500 cd/m^2
S. E. Shaheen, G. E. Jabbour, et al (2000)	Used triphenyldiamine side-group polymers as hole transport layers in multilayer organic light-emitting diodes using 8-hydroxyquinoline aluminum (Alq_3) as an emission layer.	A better performance has been observed.
Yong Qiu, Wenhua Hu et al (2000)	Comparative study of electroluminescent properties of Tris (8-hydroxyquinoline) gallium GaQ_3 and 8-hydroxyquinoline zinc (ZnQ_2)	It has been reported that the solid film of GaQ_3 could yield a very strong photoluminescence (PL) and an EL device with ZnQ_2 could harvest a higher brightness even than Alq_3 .
Zoran D. Popovic and Hany Aziz (2002)	Degradation mechanisms in small molecule-based organic light-emitting devices (OLEDs) have been reviewed	

Yoshitaka Nishio, Yuji Hamada et al (2000)	Reported the studies of small molecules which can form thin films on thermal vapor deposition.	Following properties has been reported for the EL materials: (1) Form a uniform thin film (2) Carrier (hole/electron) transport ability (3) High fluorescent yield (4) Stable to heat (have a high glass-transition temperature) (5) Suitable HOMO/LUMO levels for the carrier injections
I-Min Chan and Franklin C. Hong et al (2004)	An electrical and optical property of the NiO films deposited under various conditions has been first characterized.	NiO/ITO anode is an excellent choice to enhance the hole injection in OLED devices.
N. N. Dinh, D. V. Thanh et al (2004)	Application of the super-thin LiF layer	Enhancement in both the onset electric field (onset voltage) and the reverse current.
Naiying Du, Qunbo Mei et al (2005)	Reported that the electron-donating substituent increases the solubility of the corresponding metal quinolate complexes in nonpolar solvents and caused a red-shift in the emission wavelength.	The end groups of two compounds facilitated polymerization to form the metalloquinolate-containing polymers.
Kim, Won Sam; You, Jung Min; et al (2006)	Synthesize zinc complexes (Zn(HPB) ₂ and Zn(HPB)q)	ITO/NPB (40 nm)/Alq ₃ (60 nm)/Zn(HPB) ₂ (5 nm)/LiF/Al device showed increased luminance of L = 17000 cd/m ² compared to L = 12000 cd/m ² for similar device fabricated without the hole-blocking layer

Junfeng Xie, Juan Qiao, et al (2005)	An azomethin- zinc complex, bis[salicylidene(4-dimethylamino)aniline]zinc(II) ($Zn(sada)_2$) has been synthesized and structurally characterized	It has been found that compared with the typical bilayer device of (NPB)/tris-(8-hydroxyquinoline)aluminum (Alq_3), the device with $Zn(sada)_2$ as the electron transporting layer exhibited a much lower turn-on voltage of 2.5 V (it is usually 3.5 V for an NPB/ Alq_3 device)
Yoon-Ki Jang, Dong-Eun Kim (2006)	Synthesized new electroluminescence materials, ($Zn(HPB)_2$) and $Zn(phen)q$	The photoluminescence (PL) spectra of $Zn(HPB)_2$ and $Zn(phen)q$ has been observed to be blue and yellowish green, respectively.
Christopher Williams et al (2006)	Implemented transparent and conductive single-wall carbon nanotube sheets on the substrate.	High performance of organic light-emitting diodes (OLEDs) has been reported.
Vivek Kumar Shukla, Satyendra Kumaret et al (2006)	Annealed ITO coated substrate in oxygen near 100 °C	Sudden change in roughness which may be as a consequence of change in surface morphology due to phase change and fraction of new phase is estimated by phase images taken by AFM has been reported.
Tianzhi Yu et al (2007)	The electroluminescence devices with the ZnL (L=ligand) complex as the emitting layer have been constructed.	Blue emission with a peak at 455 nm and the maximum brightness of 650 cd m^{-2}

2.2 Scope of the work

There are a number of problems which are hindering these Zinc chelates for being utilized in OLED devices. They are life time, efficiency, operating voltage, stability. Our aim of the thesis is to improve the device performance by the following means

- Anode modification.
- Multi layer structure to increase the efficiency of OLED.
- Synthesis of novel organic emissive, hole transport, electron transport and electron injector for the enhancement of life time, efficiency and reduction in operating voltage in OLED.
- Charge confinement and interfacial engineering of OLED devices (Confinement of charge carrier and exciton is the essential factor for enhancing the efficiency and stability of the electro luminescence devices) by transport studies.

CHAPTER - 3
EXPERIMENTAL

3.1 Synthesis

3.1.1 Synthesis of Bis(8-Hydroxyquinolate)(Zinc) Znq₂:

A solution of 8-hydroxy quinoline 0.29 g (2 m mol) (Merck, India) was prepared in 40 ml absolute ethanol (s.d. Fine Chem Limited India) in a 100 ml three neck flask and stirred with a magnetic stirrer for one hour at a constant temperature of 70 °C in an oil bath. A solution of zinc acetate 0.219 g (1 m mol) in 2 ml of deionised water was added drop wise to the reaction mixture. After 2 h stirring a yellowish green precipitate of the complex was separated from the reaction mixture which was filtered and dried at 70 °C in vacuum oven for 24 h. The synthesized material was further purified by vacuum sublimation and stored in desiccators. The schematic diagram of synthesis is shown in following **Figure 3.1**.

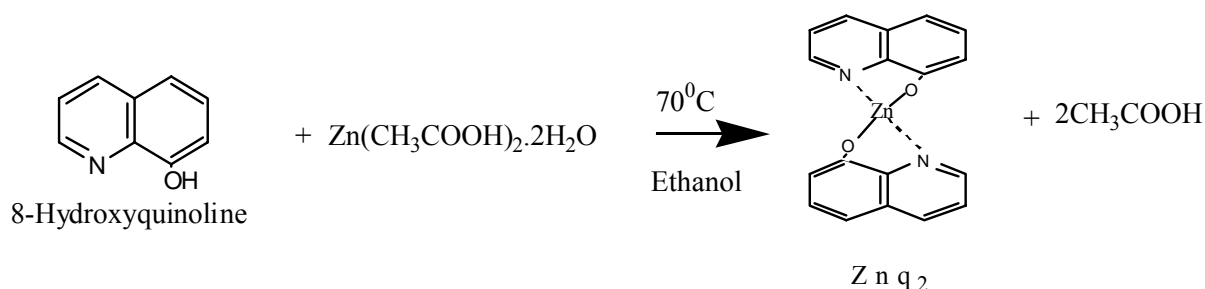


Figure 3.1: Scheme- Synthesis of Znq₂.

3.1.2 Synthesis of bis(2-methyl- 8-Hydroxyquinolate)(Zinc) Zn(mq)₂:

A solution of 2-methyl 8-hydroxy quinoline 0.32 g (2 m mol) (Merck, India) was prepared in 40 ml absolute ethanol (s.d. Fine Chem Limited India) in a 100 ml three neck flask and stirred with a magnetic stirrer for one hour at a constant temperature of 70 °C in an oil bath. A solution of zinc acetate 0.219 g (1 m mol) in 2 ml of deionised water was added drop wise to the reaction mixture. After 2 h stirring a yellowish green precipitate of the complex was separated from the reaction mixture which was filtered and dried at 70 °C in vacuum oven for 24 h. The synthesized material was further purified by vacuum sublimation and stored in desiccators. The schematic diagram of synthesis is shown in following **Figure 3.2**.

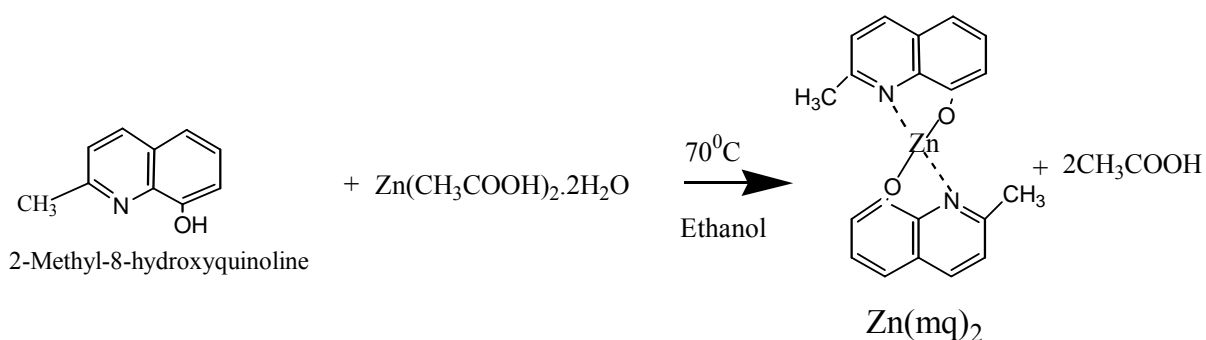


Figure 3.2: Scheme- Synthesis of Zn(mq)₂.

3.2 Material Characterization, device fabrication techniques:

3.2.1 Materials characterization

In material characterization basically we have tried to characterize the synthesized material by variety of techniques to assure that the appropriate materials with suitable properties are synthesized. Some of the characterization techniques used for the characterization of materials is described below.

3.2.1.1 UV-Visible Absorption Spectroscopy

A diagram of the components of a typical spectrometer is shown in the following diagram (**Figure 3.3**). The functioning of this instrument is relatively straightforward. A beam of light from a visible and/or UV light source (colored red) is separated into its component wavelengths by a prism or diffraction grating. Each monochromatic (single wavelength) beam in turn is split into two equal intensity beams by a half-mirrored device. One beam, the sample beam (colored magenta), passes through a small transparent container (cuvette) containing a solution of the compound being studied in a transparent solvent. The other beam, the reference (colored blue), passes through an identical cuvette containing only the solvent. The intensities of these light beams are then measured by electronic detectors and compared. The intensity of the reference beam, which should have suffered little or no light absorption, is defined as I_0 . The intensity of the sample beam is defined as I . Over a short period of time, the spectrometer automatically scans all the component wavelengths in the manner described. The ultraviolet (UV) region scanned is

normally from 200 nm to 400 nm, and the visible portion is from 400 nm to 800 nm. [47]

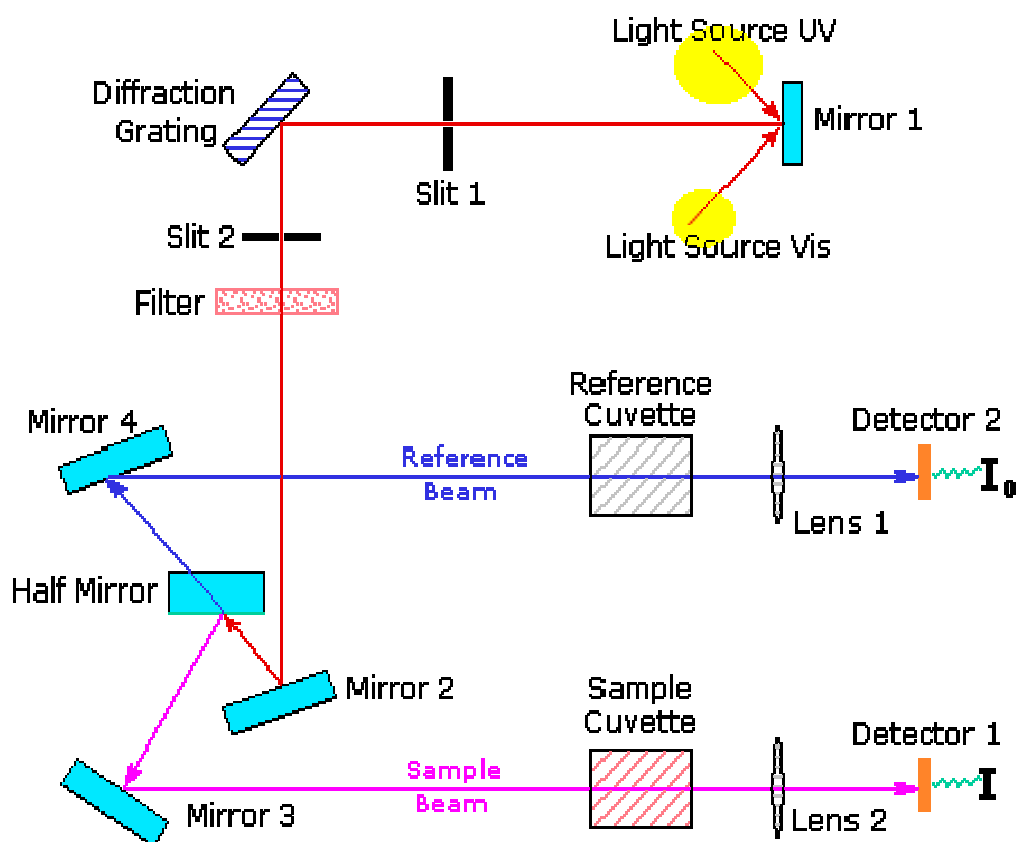


Figure 3.3: Block diagram of UV-Vis spectrometer.

If the sample compound does not absorb light of a given wavelength, $I = I_0$. However, if the sample compound absorbs light then I is less than I_0 , and this difference may be plotted on a graph versus wavelength. Absorption may be presented as transmittance ($T = I/I_0$) or absorbance ($A = \log I_0/I$). If no absorption has occurred, $T = 1.0$ and $A = 0$. Most spectrometers display absorbance on the vertical axis, and the commonly observed range is from 0 (100 % transmittance) to 2 (1 % transmittance). The wavelength of maximum absorbance is a characteristic value, designated as λ_{\max} . [48].

Principle of UV- visible spectroscopy

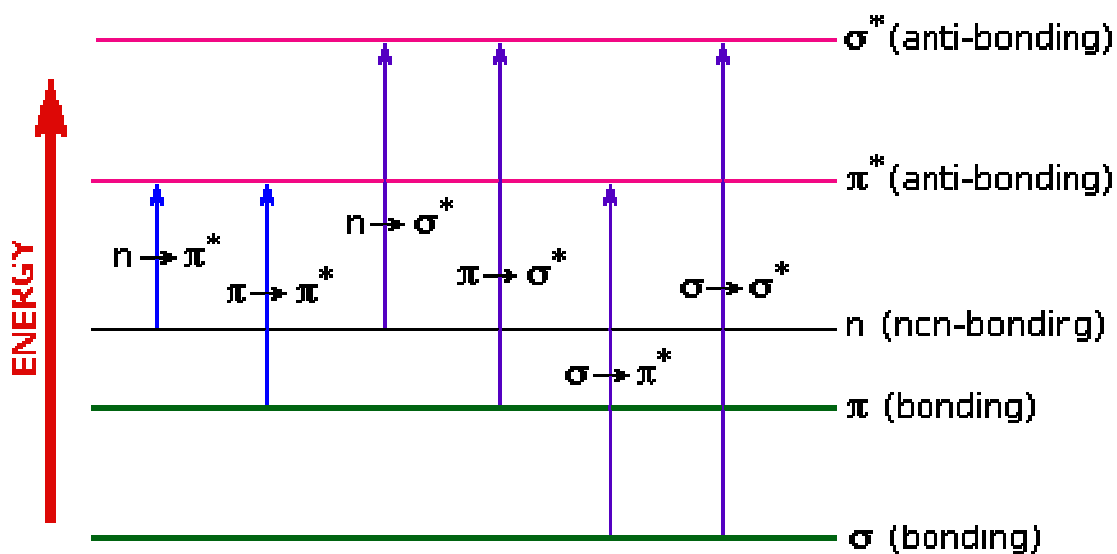


Figure 3.4: Energy level diagram.

The energies noted above are sufficient to promote or excite a molecular electron to a higher energy orbital. Consequently, absorption spectroscopy carried out in this region is sometimes called "electronic spectroscopy". A diagram showing the various kinds of electronic excitation that may occur in organic molecules is shown in **Figure 3.4**. Of the six transitions outlined, only the two lowest energy ones (left-most, colored blue) are achieved by the energies available in the 200 to 800 nm spectrum. As a rule, energetically favored electron promotion will be from the highest occupied molecular orbital (HOMO) to the lowest unoccupied molecular orbital (LUMO), and the resulting species is called an excited state [49].

When sample molecules are exposed to light having an energy that matches a possible electronic transition within the molecule, some of the light energy will be absorbed as the electron is promoted to a higher energy orbital. An optical spectrometer records the wavelengths at which absorption occurs, together with the degree of absorption at each wavelength. Because the absorbance of a sample will be proportional to the number of absorbing molecules in the spectrometer light beam (e.g. their molar concentration in the sample tube), it is necessary to correct the absorbance value for this and other operational factors if the spectra of different compounds are to be compared in a meaningful way. The corrected absorption value is called "molar absorptivity", and is particularly useful when comparing the spectra of different

compounds and determining the relative strength of light absorbing functions (chromophores). **Molar absorptivity** (ϵ) is defined as

Molar Absorptivity, $\epsilon = A / c l$, Where A= absorbance,

c = sample concentration in moles/liter & **l** = length of light path through the sample in cm

3.2.1.2 Photoluminescence Spectroscopy

Photoluminescence spectroscopy (Schematic diagram in **Figure 3.5**) is a contactless, non destructive method of probing the electronic structure of materials. Light is directed onto a sample, where it is absorbed and imparts excess energy into the material in a process called photo-excitation. One way this excess energy can be dissipated by the sample is through the emission of light, or luminescence. In the case of photo-excitation, this luminescence is called photoluminescence. The intensity and spectral content of this photoluminescence is a direct measure of various important material properties. Photo-excitation causes electrons within the material to move into permissible excited states. When these electrons return to their equilibrium states, the excess energy is released and may include the emission of light (a radiative process) or may not (a nonradiative process). The energy of the emitted light (photoluminescence) relates to the difference in energy levels between the two electron states involved in the transition between the excited state and the equilibrium state. The quantity of the emitted light is related to the relative contribution of the radiative process. [50].

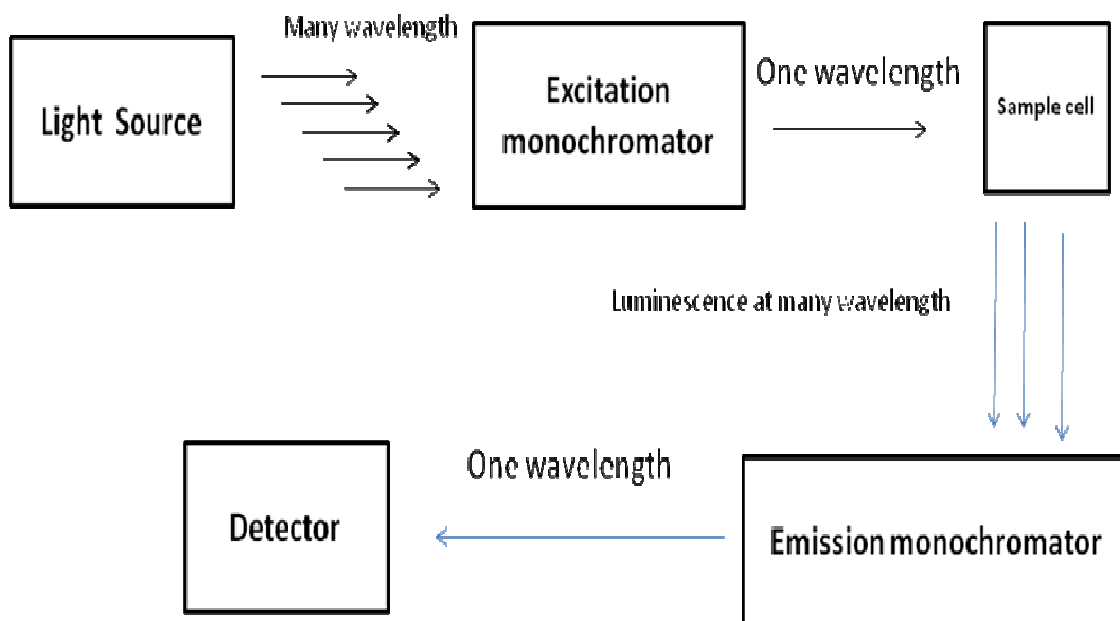


Figure 3.5: Schematic diagram of luminescence experiment

3.2.1.3 Fourier Transforms Infra-Red (FT-IR) Spectroscopy

A molecule absorbs radiation only when the natural frequency of vibration of some part of molecule (i.e. atoms or group of atoms comprising it) is the same as the frequency of the incident radiation. After absorbing the correct wavelength of radiation, the molecule vibrates at increased amplitude. This occurs at the expense of the energy of the IR radiation, which has been absorbed.

Infrared spectroscopy is one of the most powerful analytical technique, which offers the possibility over the other usual method of structural analysis (X-ray diffraction, electron spin resonance, etc) is that its provides useful information about the structure of the molecules and bonding quickly, without tore-some evaluation method. Moreover, FT-IR provides a very faster of identifying chemical structures especially those of the organic ones.

FT-IR spectroscopy employs an interferometer in place of monochromatic (**Figure 3.6**). This device generates the Fourier transform of the infera-red spectrum, which is converted to spectrum itself by a computer. This approach has the advantageous of providing much higher source radiation throughput, increased signals-to-noise (S/N) ratio and higher wave number accuracy than is possible with a conventional light dispersive spectrometer [49].

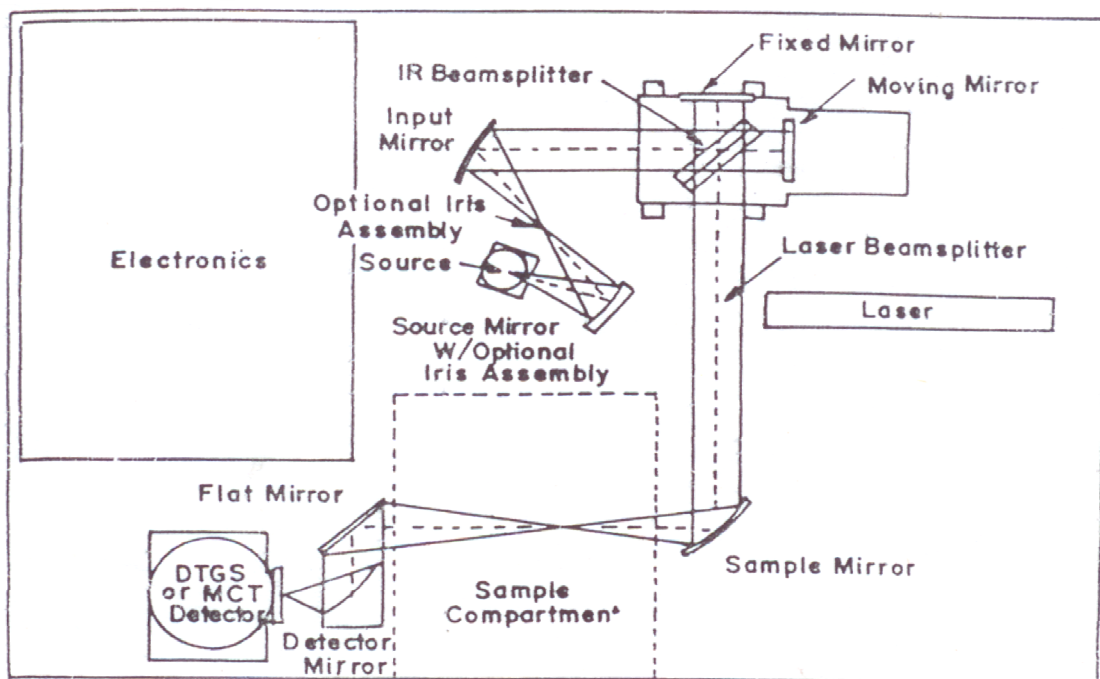


Figure 3.6: Set-up of FT-IR (model 510p).

The technique is based upon the simple fact that a chemical substance shows marked selective absorption in infrared region giving rise to close-packed absorption bands, called an IR absorption spectrum, which may extend over a wide wavelength range. Various bands in an IR spectrum correspond to characteristic functional groups and bonds present in the chemical substance. IR spectrum of a chemical substance is thus a fingerprint for its identification. Band position in infrared spectrum may be expressed conveniently by wave number $\tilde{\nu}$, whose unit is cm^{-1} . The relation between velocity c , wavelength λ and frequency $\tilde{\nu}$ is as follows;

$$\tilde{\nu} = c/\lambda \text{ or } \tilde{\nu}/\text{cm}^{-1} = 1/\lambda$$

Band intensities in IR spectrum may be expressed either as transmittance (T) or absorbance (A). Transmittance is defined as the ratio of the radiant power transmitted by a sample to the radiant power incident on the sample. In most spectrums transmittance (T) versus wave number (cm^{-1}) has been plotted.

3.2.1.4 Thermo Gravimetric Analysis

Thermo Gravimetric Analysis (TGA) is a thermal analysis technique used to measure changes in the weight (mass) of a sample as a function of temperature and/or time. TGA is commonly used to determine polymer degradation temperatures, residual solvent levels, absorbed moisture content, and the amount of inorganic (noncombustible) filler in polymer or composite material compositions.

A simplified explanation of a TGA sample evaluation may be described as follows. A sample is placed into a tarred TGA sample pan which is attached to a sensitive microbalance assembly. The sample holder portion of the TGA balance assembly is subsequently placed into a high temperature furnace. The balance assembly measures the initial sample weight at room temperature and then continuously monitors changes in sample weight (losses or gains) as heat is applied to the sample. TGA tests may be run in a heating mode at some controlled heating rate, or isothermally. Typical weight loss profiles are analyzed for the amount or percent of weight loss at any given temperature, the amount or percent of noncombusted residue at some final temperature, and the temperatures of various sample degradation processes [51].

3.2.2 Device Fabrication Techniques

Fabrications of a OLED includes the deposition of a thin film (polymer or small molecules) over a glass substrate which is already coated with Indium tin Oxide (ITO) which is the anode and a low work function metal is the cathode. Typically organic layer thickness is nearly 100 nm. A deposited thin film is a layer on a surface having properties that differ from those of the bulk material (substrate) that has been formed by the addition of solid materials to the surface. Generally, the substrate material cannot be detected in the film, which can be an organic or inorganic material. This surface layer differs from surface conversion where the surface is chemically converted to another material, e.g., anodization of aluminium. The term thin film is generally applied to layers that have thicknesses on the order of several micrometers or less. These films may be as thin as a few atomic layers. In many cases, adding atoms or molecules to a substrate surface one at a time forms thin films. Thicker layers are generally called coatings. Although the same processes that are used to form thin films can often form coatings, there are some coating processes that are not applicable to forming thin films. For example, thermal spray coating processes, which

melt small particles, accelerate them to high velocities, and splat-cool them on the surfaces, are not applicable to forming thin films. The properties of thin films generally differ from the values for the materials in the bulk form. In many cases, the growth and properties of thin films are affected by the properties of the underlying substrate material. The properties of the film can also be affected by the high surface to volume ratio of the film. Many techniques are used for device fabrication, one of them we used for device fabrication was vacuum evaporation technique. Before preparing a device its patterning is very important. To obtain desired patterns from OLEDs the layer of ITO on glass surface is shaped in a certain manner. It is achieved by Photolithography.

Vacuum evaporation techniques:

Vacuum deposition, some time called vacuum evaporation technique, is a major physical deposition technique that is extensively used for the deposition of thin films on the surface of a substrate. The vacuum thermal evaporation deposition technique consists in heating until evaporation of the material to be deposited. The material vapor finally condenses in form of thin film on the cold substrate surface and on the vacuum chamber walls. Usually low pressures are used (about 10^{-6} or 10^{-5} Torr), to avoid reaction between the vapor and atmosphere. At these low pressures, the mean free path of vapor atoms is the same order as the vacuum chamber dimensions, so these particles travel in straight lines from the evaporation source towards the substrate. This originates 'shadowing' phenomena with 3D objects, especially in those regions not directly accessible from the evaporation source (crucible). Besides, in thermal evaporation techniques the average energy of vapor atoms reaching the substrate surface is generally low (i.e. kT , order of tenths of eV). This affects seriously the morphology of the films, often resulting in a porous and little adherent material. In thermal evaporation techniques, different methods can be applied to heat the material. The equipments available in the laboratory use either resistance heating (Joule effect) or bombardment with a high-energy electron beam, usually several KeV, from an electron beam gun (electron beam heating). The principal processing variables in vacuum deposition are deposition geometry, deposition rate, and substrate temperature during deposition and the level of gaseous and vapor (e.g., water vapor) contamination in the deposition environment. Deposition rates and amounts can be monitored in situ and in real-time by oscillation frequency to change. Calibration

allows the change in frequency to be related to deposited film mass and by assuming a film density, the film thickness. In many applications the amount of material deposited is controlled by the evaporation-to-completion of a specific amount of material and using specific deposition geometry. In many cases a property of thin film, such as optical transmittance, is monitored during deposition and is controlled the amount of material deposit.

3.3 Device Fabrication

3.3.1 Znq₂ and Zn(mq)₂ based Organic Light Emitting Device:

The OLED device was fabricated in a configuration ITO/ α -NPD (40 nm)/Znq₂orZn(mq)₂ (35 nm)/BCP(6 nm)/Alq₃(30 nm)/LiF(1 nm)/Al(100 nm)(as shown in schematic diagram of OLED Device **Figure 3.7**). Indium-tin oxide (ITO) coated glass substrates with sheet resistance of 20 Ω/\square were patterned using photolithography and cleaned using trichloroethylene, acetone, isopropyl alcohol and deionised water sequentially for 20 minutes using an ultrasonic bath and dried in flowing nitrogen. Prior to film deposition, the ITO substrates were treated with oxygen plasma for 5 minute. On the substrate, the hole transport layer and the emitting layers were deposited sequentially under a high vacuum (1×10^{-5} torr) at a deposition rate of 0.2 - 0.5 $\text{\AA}/\text{sec}$ and LiF at 0.1-0.2 $\text{\AA}/\text{sec}$. Thickness of the deposited layers were controlled by a quartz crystal monitor. The cathode was deposited on the top of the structure through a shadow mask. A 40 nm N,N diphenyl-N'N'-bis(1-naphthyl)-1,1'-biphenyl-4,4'-diamine(α -NPD) (Sigma Aldrich) was used as hole transport layer. Znq₂ or Zn(mq)₂ was used as the emitting layer and aluminium tris-8-hydroxyquinoline(Alq₃) (Sigma Aldrich) was used as electron transport layer. The electron injection was facilitated using a 1nm thin LiF (Merck, Germany) layer followed by a thick layer of Aluminium. The size of each pixel was $5 \times 5 \text{ mm}^2$.

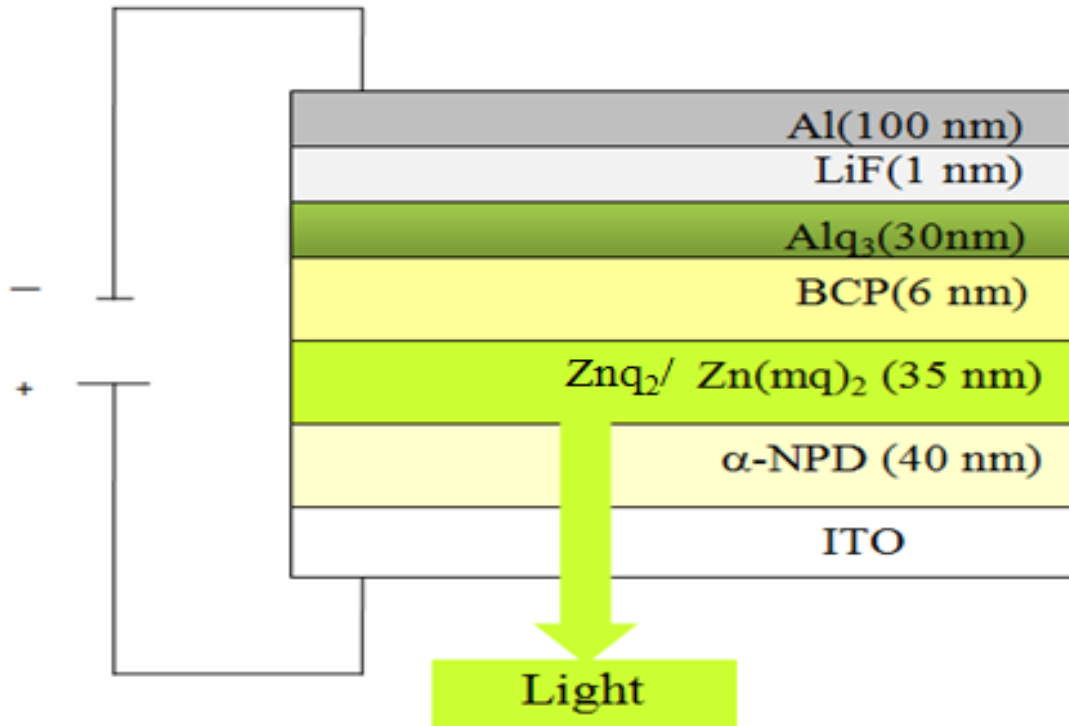


Figure 3.7: Device structure of OLED ($\text{Znq}_2/\text{Zn(mq)}_2$ as an emitter).

The luminance–current–voltage (I-V-L) characteristics were measured using a luminance meter (LMT 1009) and a Keithley 2400 programmable voltage-current digital source meter.

3.3.2 Hole-only Devices Based on Znq_2 and Zn(mq)_2 materials for transport Studies:

To study the hole transport behaviour of both the materials (Znq_2 and Zn(mq)_2) we have also fabricated the devices on a ITO/ Znq_2 (250 nm)/Au(350 nm) and ITO/ Zn(mq)_2 (250 nm)/Au(350 nm) configurations respectively (**Figure 3.8**).

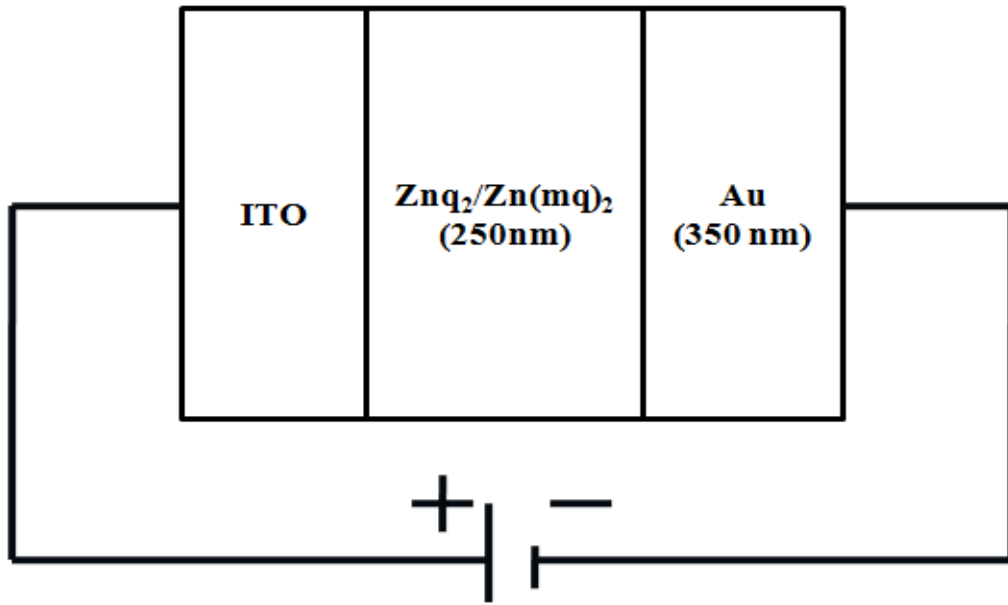


Figure 3.8: Hole-Only device.

CHAPTER - 4
RESULTS AND DISCUSSION

4.1 Structural and thermal characterization

The infrared absorption spectrum of the material in KBr pellets has been studied using a Nicolet 5700 Spectrometer. The Thermo Gravimetric Analysis (TGA) has been done by using SDTA851e Metter-Toledo-star system in the temperature range 0 - 600 °C.

4.1.1 Structural and thermal characterization of Znq₂

Following **Figure 4.1** shows the FTIR spectrum of the material carried out on sample, prepared by pellets containing Zn(mq)₂ powder (0.1 weight %) dispersed in KBr powder. The spectrum shows the characteristics peaks of aromatic ring stretching at 740 cm⁻¹, 787 cm⁻¹ and 819 cm⁻¹, which is due to the existence of quinolinic rings. The peak at 1573 cm⁻¹ is indicative peak of C=C aromatic stretching. Aromatic amine resonance peak of C-N-C at 1279 cm⁻¹ and 1371 cm⁻¹, C=N stretching at 1421 cm⁻¹ and aromatic C-O stretching at 1105 cm⁻¹ were observed in the spectrum.

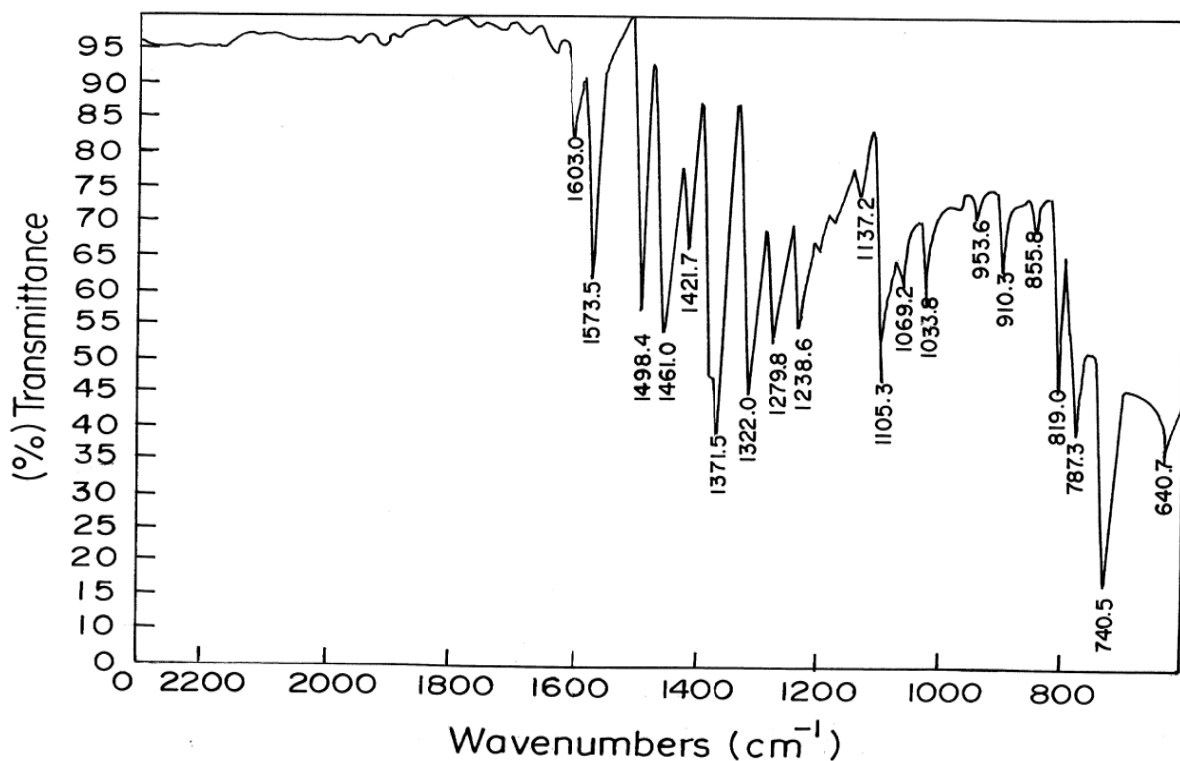


Figure 4.1: FTIR spectrum of Znq₂.

TGA of synthesized Znq_2 was carried out in the temperature range 0-600 °C as shown in **Figure 4.2**. The TGA plot of Znq_2 shows a large weight loss which starting from 350 °C indicating thermal degradation. This shows that the compound was stable up to 350 °C. The high thermal stability in nitrogen is attributed to the highly polarized Zn-N bond. The high thermal stability of Znq_2 is as an advantage in the fabrication of organic light emitting device for getting greater longevity.

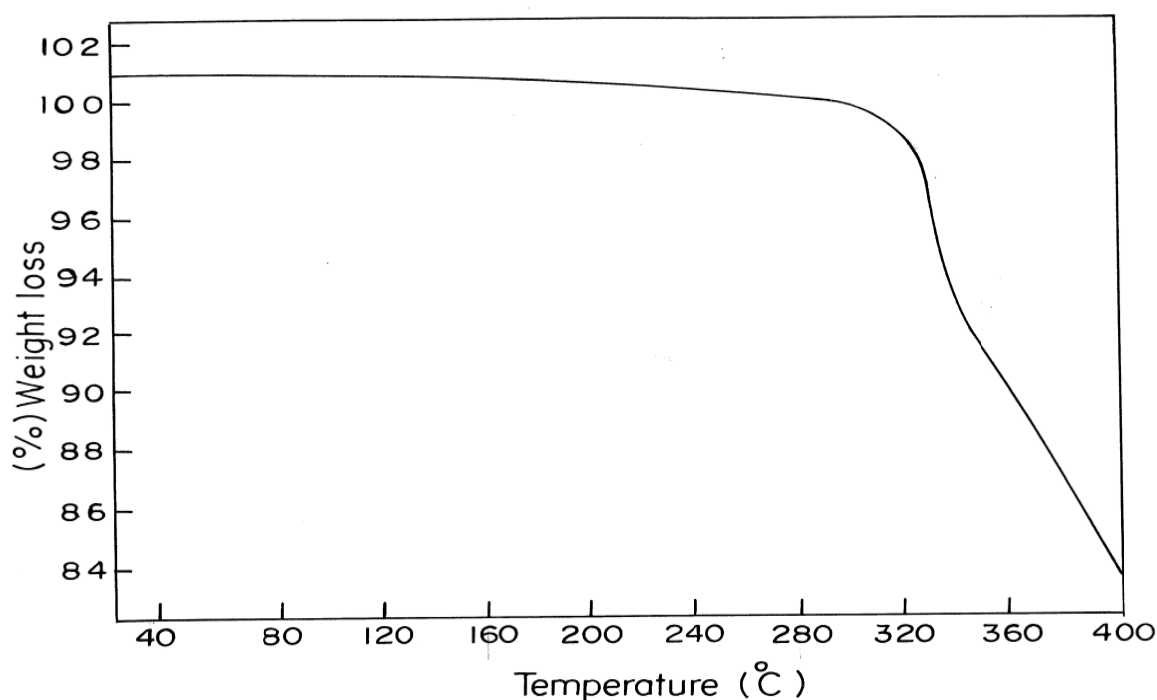


Figure 4.2: Thermo Gravimetric Analysis (TGA) of Znq_2 .

4.1.2 Structural and thermal characterization of Zn(mq)_2

Following **Figure 4.3** shows the FTIR spectrum of the material carried out on sample, prepared by pellets containing Zn(mq)_2 powder (0.1 weight %) dispersed in KBr powder. The spectrum shows the characteristics peaks of aromatic ring stretching at 747 cm^{-1} , 830 cm^{-1} and 874 cm^{-1} , which is due to the existence of quinolinic rings. The peak at 1564 cm^{-1} is indicative peak of C=C aromatic stretching. Aromatic amine resonance peak of C-N-C at 1278 cm^{-1} and 1306 cm^{-1} , C=N stretching at 1421 cm^{-1} and aromatic C-O stretching at 1106 cm^{-1} were observed in the spectrum. Peak

observed at 3035 cm^{-1} in the spectrum is the characteristic peaks for aromatic C-H stretching, which confirm the presence of methyl group.

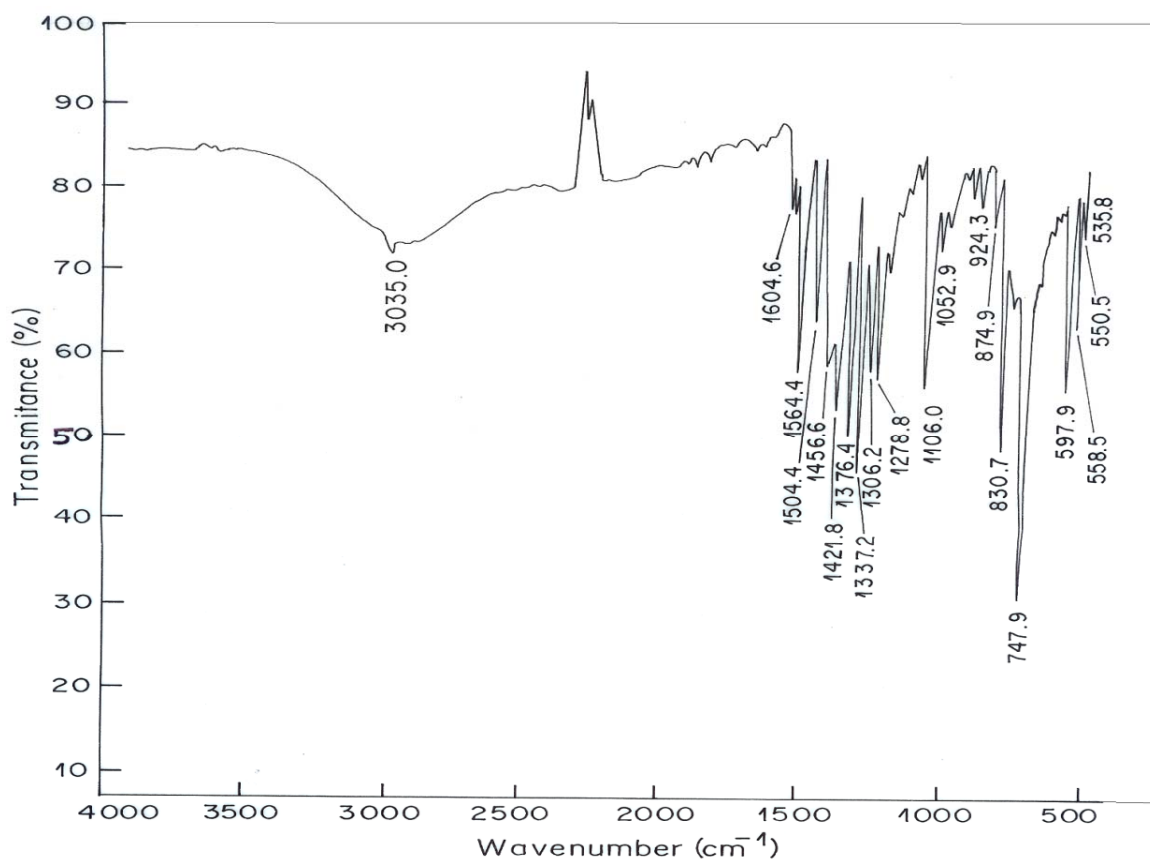


Figure 4.3: FTIR spectrum of $\text{Zn}(\text{mq})_2$.

TGA of synthesized $\text{Zn}(\text{mq})_2$ was carried out in the temperature range $0\text{--}600\text{ }^\circ\text{C}$ as shown in **Figure 4.4**. The TGA plot of $\text{Zn}(\text{mq})_2$ shows a large weight loss which starting from $330\text{ }^\circ\text{C}$ indicating thermal degradation. This shows that the compound was stable up to $330\text{ }^\circ\text{C}$. The high thermal stability in nitrogen, which is attributed to the highly polarized Zn-N bond. The high thermal stability of $\text{Zn}(\text{mq})_2$ is as an advantage in the fabrication of organic light emitting device for getting greater longevity.

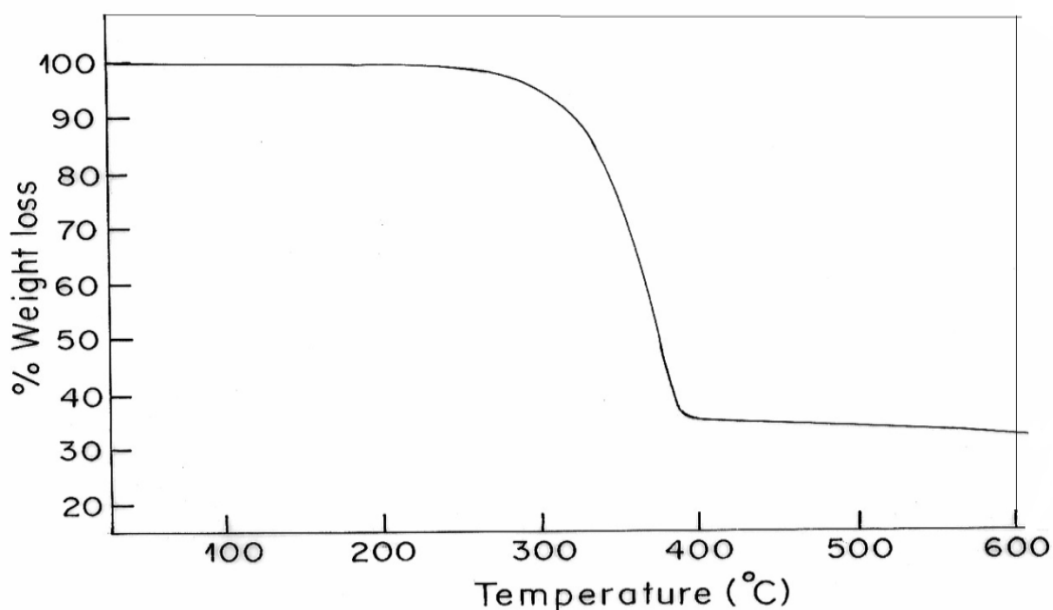


Figure 4.4: Thermo Gravimetric Analysis (TGA) of Zn(mq)₂.

4.2 Optical characterization

UV-visible absorption spectra were recorded on a Shimadzu UV-2401 spectrophotometer. The excitation and emission spectra of a thin film of Zn(mq)₂ were recorded with a Fluorolog Spectrofluorometer (Horiba Jobin YVON Fluolog Model FL 3-11) at room temperature.

4.2.1 Optical characterization of Znq₂

The UV-Vis absorption and photoluminescence spectrum were obtained in a thin film of Znq₂ and are shown in **Figure 4.5**. The maximum of the UV-Vis absorption peaks of Znq₂ was observed at 380 nm, which is due to the π - π^* transition of aromatic ring. The peak of the PL spectrum of Znq₂ was observed at 542 nm. The quantum yield of Znq₂, was measured as 41 %. For this measurement a thin film (100 nm) of Znq₂ was deposited by the thermal vapour evaporation technique at high vacuum (1×10^{-5} torr). Extinction coefficient of Znq₂ was measured as $7.788 \times 10^3 \text{ moles}^{-1} \text{LCm}^{-1}$.

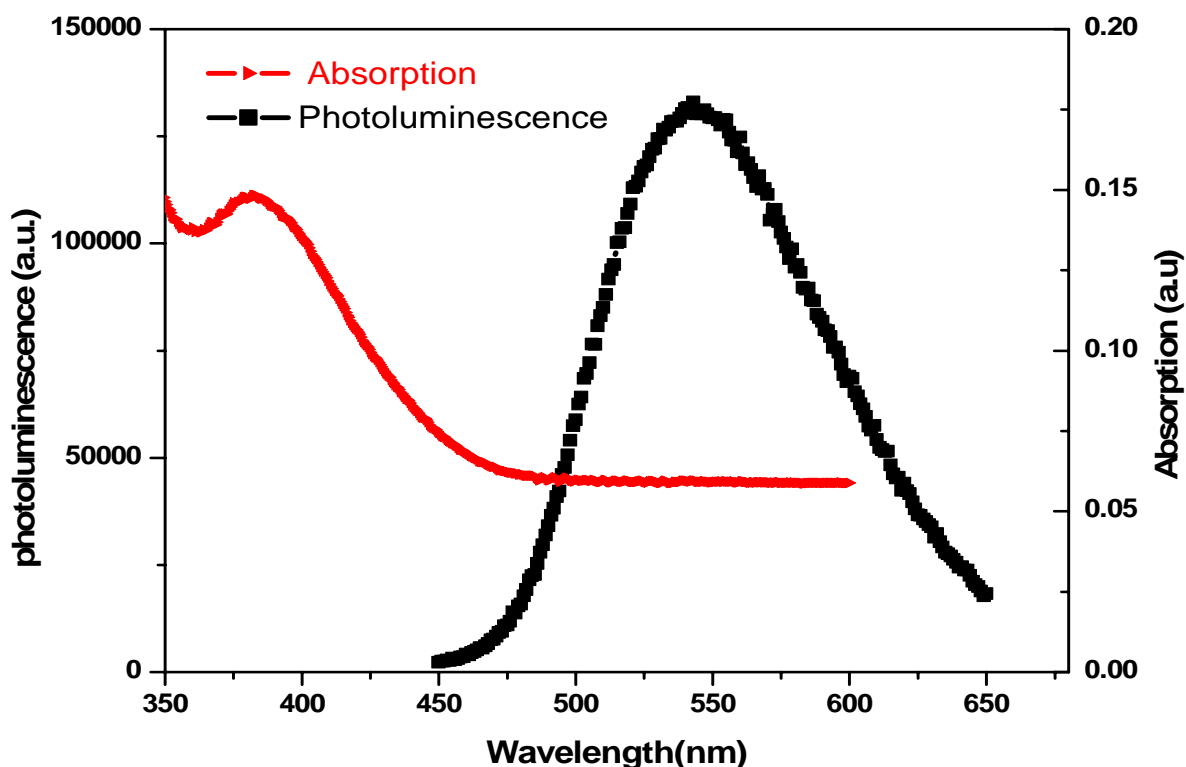


Figure 4.5: UV-Visible and Photoluminescence spectrum of Znq₂.

4.2.2 Optical characterization of Zn(mq)₂

The UV-Vis absorption and photoluminescence spectrum were obtained in a thin film of Zn(mq)₂ and are shown in **Figure 4.6**. The maximum of the UV-Vis absorption peaks of Zn(mq)₂ were observed at 385 nm, which is due to the π - π^* transition of aromatic ring. The peak of the PL spectrum of Zn(mq)₂ was observed at 530 nm. The quantum yield of Zn(mq)₂, was measured as 21 %. For this measurement a thin film (100nm) of Zn(mq)₂ was deposited by the thermal vapour evaporation technique at high vacuum (1×10^{-5} torr). Extinction coefficient of Zn(mq)₂ was measured as $1.869 \times 10^3 \text{ moles}^{-1} \text{LCm}^{-1}$.

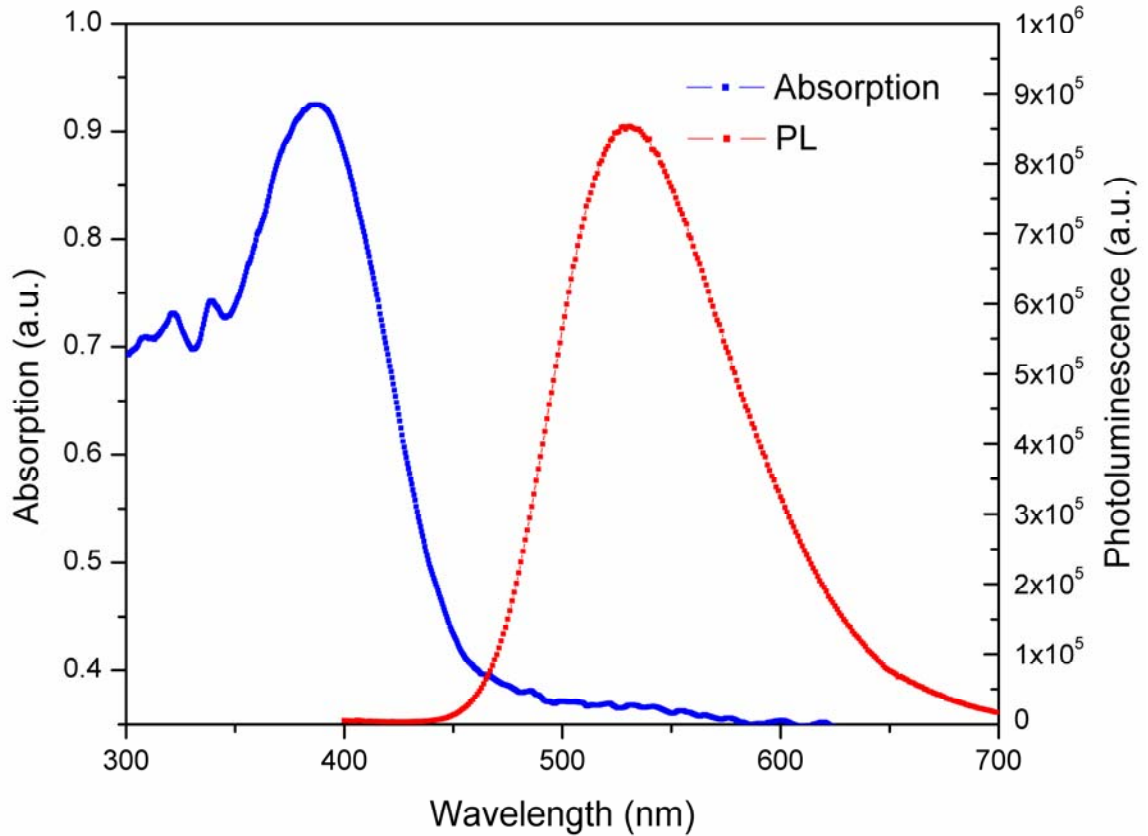


Figure 4.6: UV-Visible and Photoluminescence spectrum of Zn(mq)₂.

4.3 Device characterization

The electroluminescent (EL) spectrum was recorded on a high-resolution spectrometer (Ocean Optics, HR-2000CG UV-NIR). The luminance–current–voltage (I-V-L) characteristics were measured using a luminance meter (LMT 1009) and a Keithley 2400 programmable voltage-current digital source meter.

4.3.1 Device characterization of Znq₂

The EL spectra were recorded at various applied voltages (**Figure 4.7**). It was observed that the EL spectrum is similar to PL a spectrum which indicates that the EL and PL have the same origin. The EL intensity of the device increases with increase in voltage from 11 V to 15 V, and the peak position remain unchanged at 558 nm.

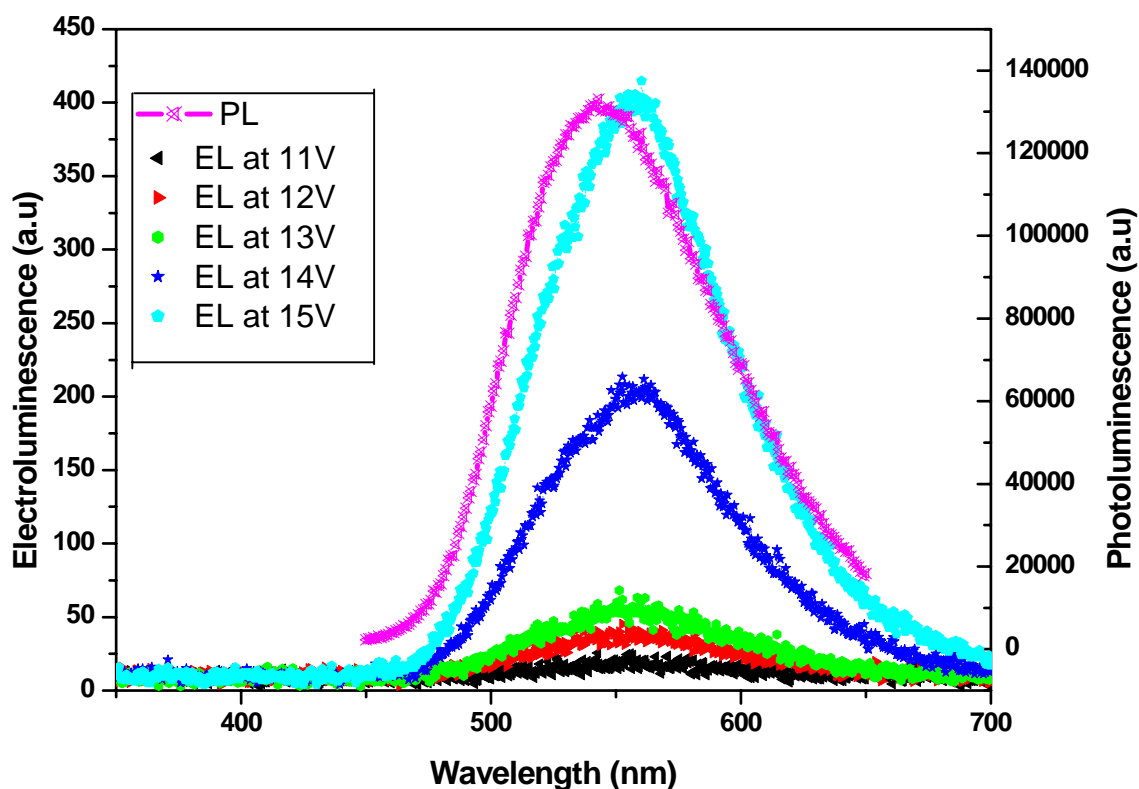


Figure 4.7: Photoluminescence and Electroluminescence spectra at different voltages.

The current voltage (I-V) characteristic of the fabricated device was recorded by applying voltage across the device with ITO as an anode and Aluminium as cathode (forward bias) as shown in **Figure 4.8**. From the I-V characteristic it has been seen that the onset of light emission starts at about 10.5 V (threshold voltage). Above this voltage, the current rises non-linearly due to the space charge effects. Above the threshold voltage the device emits a yellowish light. Below this voltage the I-V characteristics shows Ohmic current indicating the presence of thermally generated carrier.

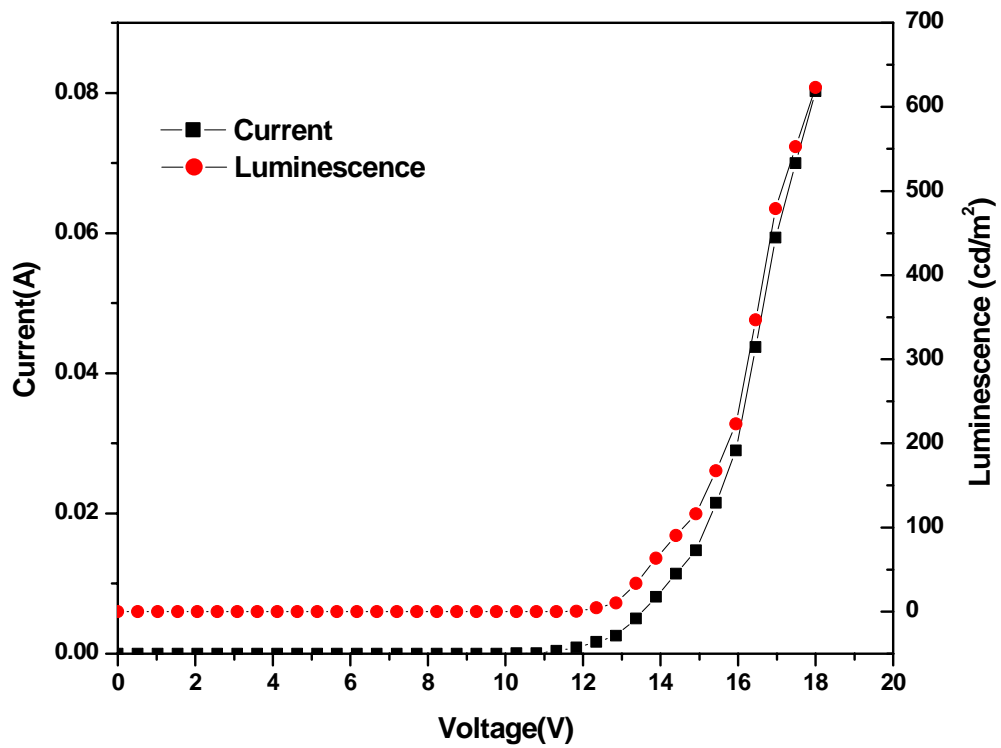


Figure 4.8: I-V-L characteristics of the device.

The maximum luminance in the EL cell was 623 cd/m^2 at 18 V with current density of 5013 A/m^2 (**Figure 4.9**). The device shows maximum current efficiency 0.12 cd/A and maximum power efficiency 0.028 lm/W at 13 V.

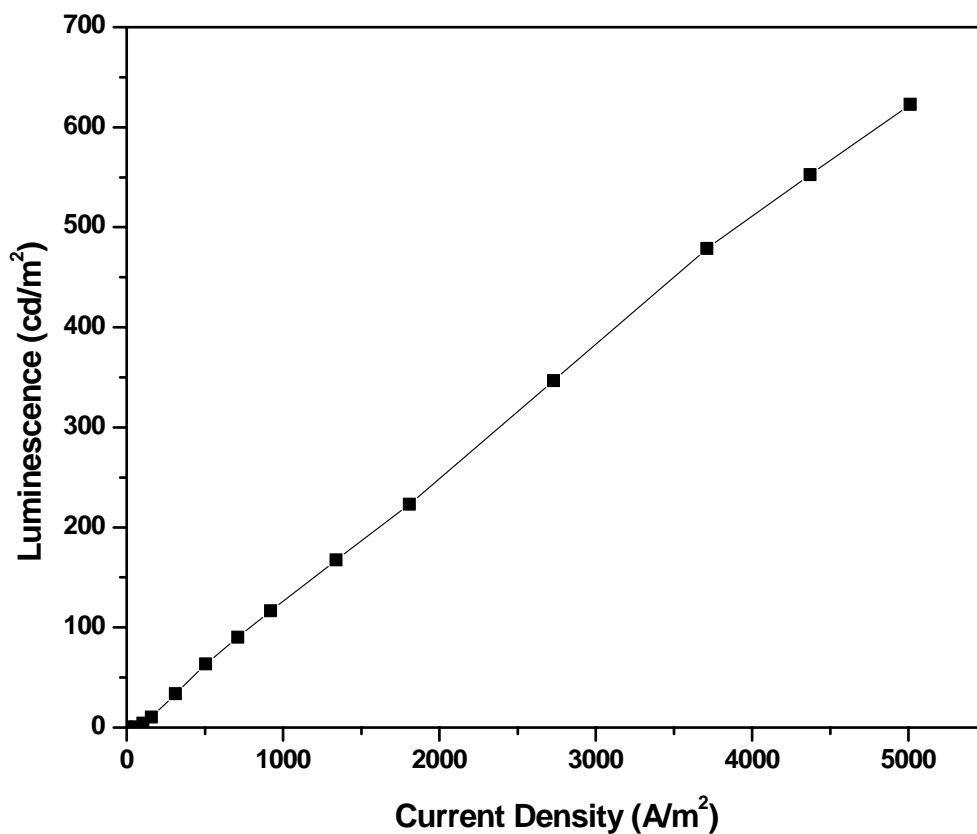


Figure 4.9: J-L characteristics of the device.

4.3.2. Device characterization of $Zn(mq)_2$

The EL spectra were recorded at various applied voltages (**Figure 4.10**). It was observed that the EL spectrum is similar to PL spectrum which indicates that the EL and PL have the same origin. The EL intensity of the device increases with increase in voltage from 5 V to 10 V, and the peak position remain unchanged at 540 nm.

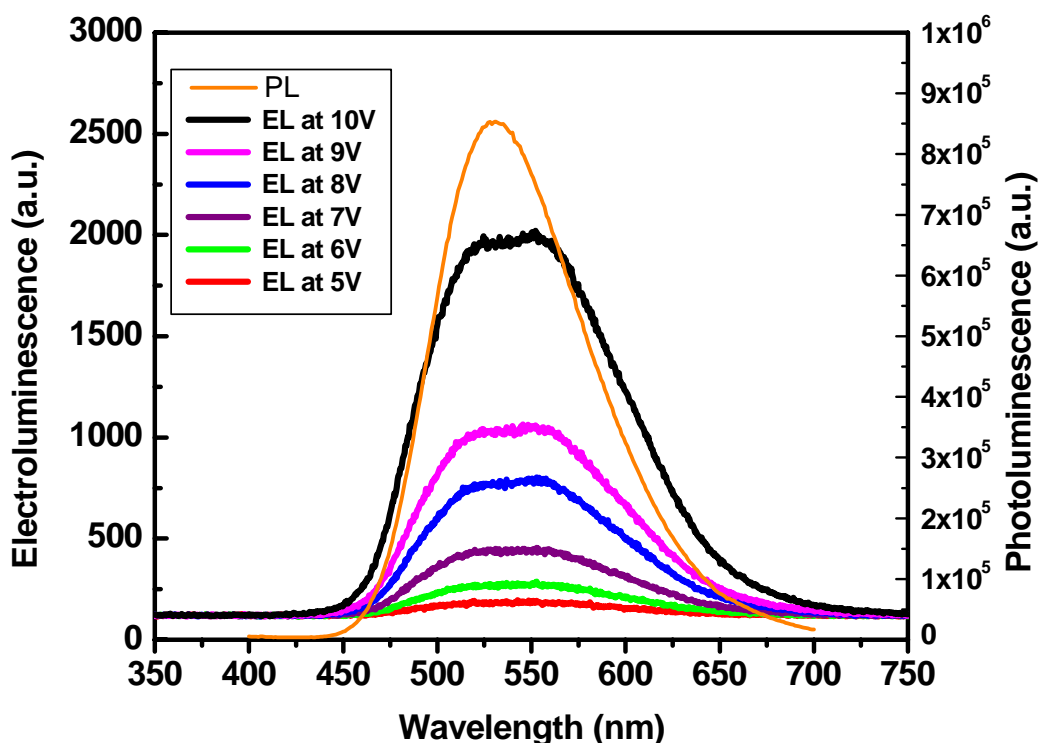


Figure 4.10: Photoluminescence and Electroluminescence spectra at different voltages.

The current voltage (I-V) characteristic of the fabricated device was recorded by applying voltage across the device with ITO as an anode and Aluminium as cathode (forward bias) as shown in **Figure 4.11**. From the I-V characteristic it has been seen that the onset of light emission starts at about 4.5 V (threshold voltage). Above this voltage, the current rises non-linearly due to the space charge effects. Above the threshold voltage the device emits a yellowish green light. Below this voltage the I-V characteristics shows Ohmic current indicating the presence of thermally generated carrier.

The maximum luminance in the EL cell was 752 cd/m^2 at 18 V with current density of 3200 A/m^2 **Figure 4.12**. The device shows maximum current efficiency 0.30 cd/A and maximum power efficiency 0.12 lm/W at 8 V.

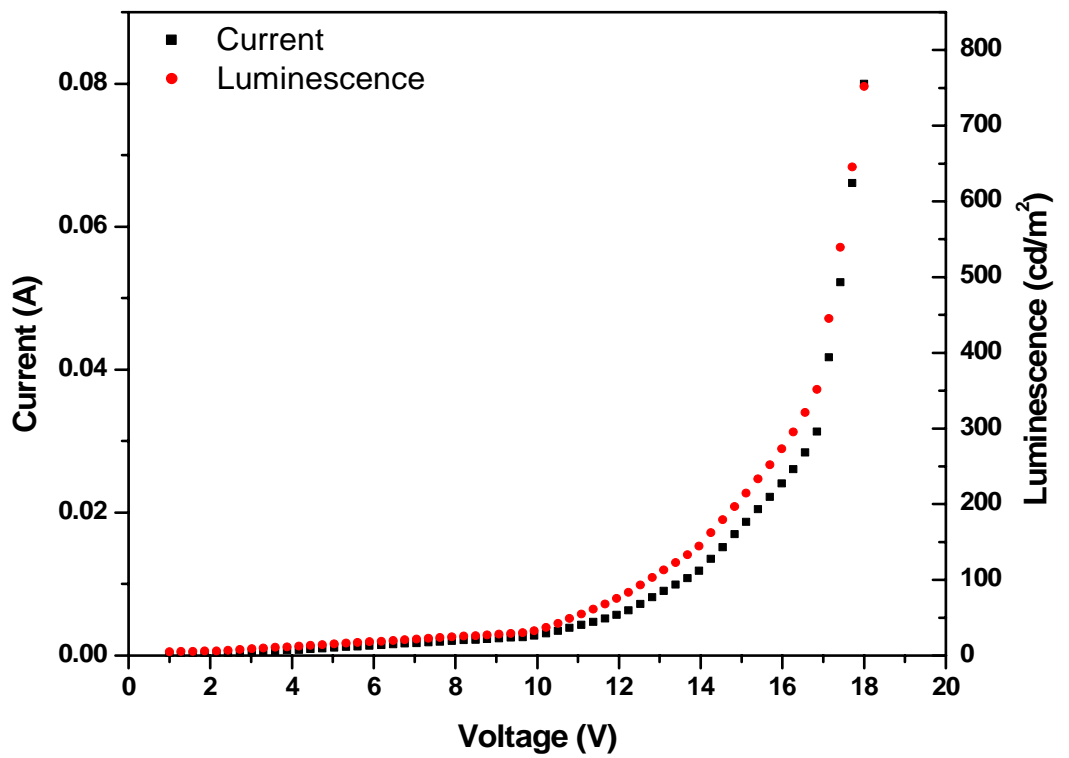


Figure 4.11: I-V-L characteristics of the device.

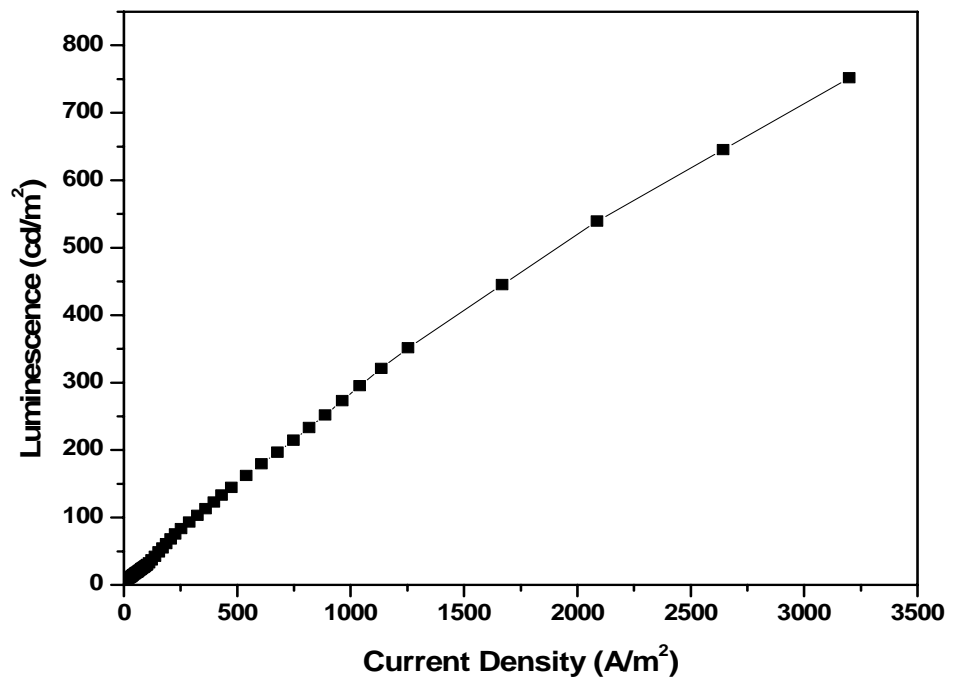


Figure 4.12: J-L characteristics of the device.

4.4 Low Temperature I-V measurement and Transport Studies

I-V characteristics of metal/semiconductor/metal devices are controlled by two basic processes: (a) injection of charge carriers from electrodes into the semiconductor layer; and (b) transport of charge carriers in the bulk of the film.

The tunnelling mechanism for charge injection predicts that the current is temperature independent and depends on the electric field. The Fowler-Nordheim (FN) tunnelling model predicts that at large forward bias the current is given by

$$j_{FN} = BF^2 \exp \left[-\frac{b}{F} \right] \dots\dots\dots (1)$$

$$\text{Where } B = \frac{e^3}{8\pi h \Delta}$$

Here e is the elementary charge, h the Planck constant, and m* the effective mass of the carrier inside the dielectric.

where F is the electric field strength and b is a parameter that depends on the barrier shape. If the injected charge is assumed to be tunnelling through a triangular barrier, the constant b in Eq. (1) is given by

$$b = \left[\frac{8\pi(2m^*)^{1/2}\Delta^{3/2}}{3he} \right] \dots\dots\dots (2)$$

where Δ is the Schottky energy barrier, m* is the effective mass of the charge carriers, q is the magnitude of the electronic charge, and h is Planck's constant.

Now solving equation (1), we get

$$\ln \left(\frac{J}{F^2} \right) = - \left[\frac{8\pi(2m^*)^{1/2}\Delta^{3/2}}{3he} \right] \frac{1}{F} + C \dots\dots\dots (3)$$

4.4.1 Transport Studies of Znq₂

From the low temperature I-V measurements of Znq₂, current is found to be temperature independent, and it is injection limited by tunnelling mechanism (as shown in **Figure 4.13**). So we have plotted $\ln (J/F^2)$ vs $1/F$ to calculate the injection barrier height.

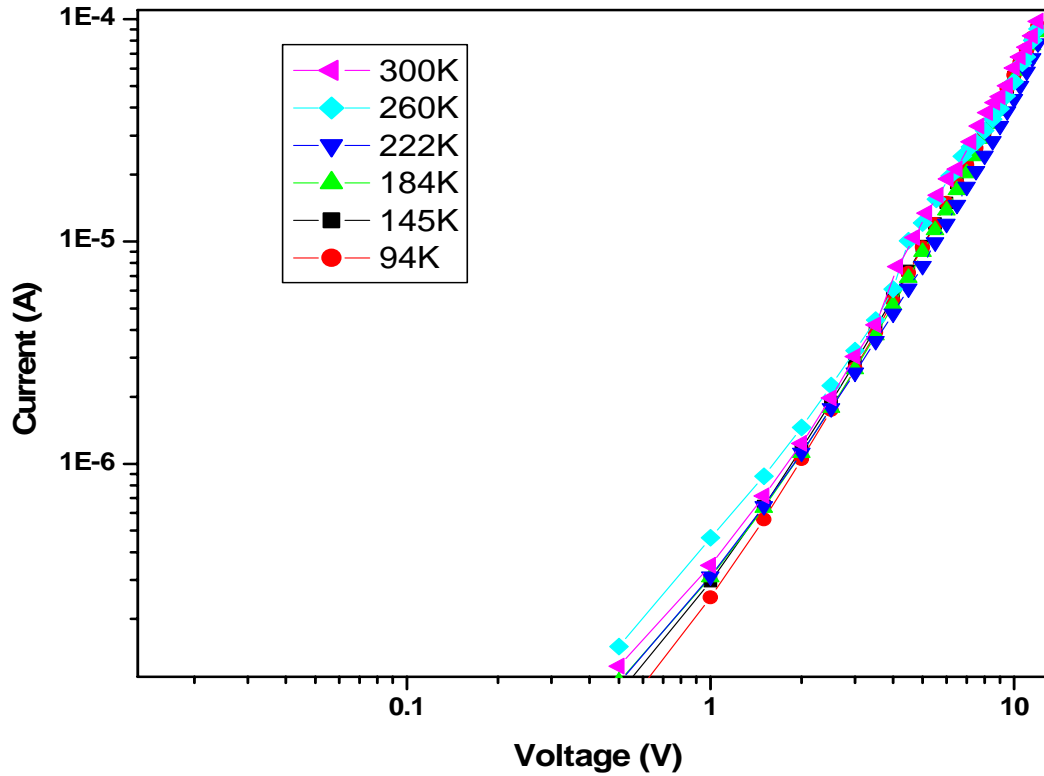


Figure 4.13: Current-Voltage characteristics of the device showing temperature independent behaviour.

The Fowler-Nordheim plot, $\ln(J/F^2)$ vs $1/F$ is shown in **Figure 4.14**. The plot is very close to linear at high field, indicating tunnelling [52]. The deviation from linearity at high voltage is due to the series resistance of the device and degradation of the device arising from Joule heating and that at lower field was thought to be due to a thermionic emission contribution to the current [52, 53]. The barrier height can be obtained from the FN formula [54] using Eqs. (1) and (3). The barrier height is calculated to be 0.025 eV.

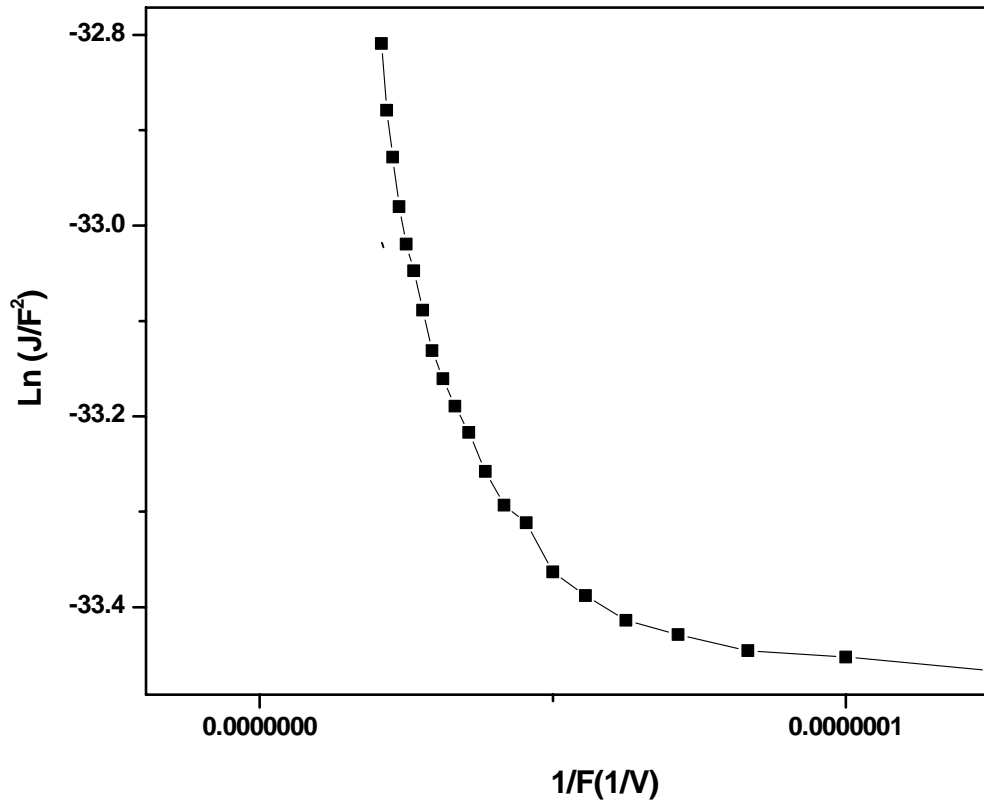


Figure 4.14: The Fowler-Nordheim plot, $\ln(I/F^2)$ vs $1/F$, of Znq_2 device

4.4.2 Transport Studies of $Zn(mq)_2$

From the low temperature I-V measurements of Znq_2 , current is found to be temperature independent, and it is injection limited by tunnelling mechanism (as shown in **Figure 4.15**). So we have plotted $\ln(J/F^2)$ vs $1/F$ to calculate the injection barrier height.

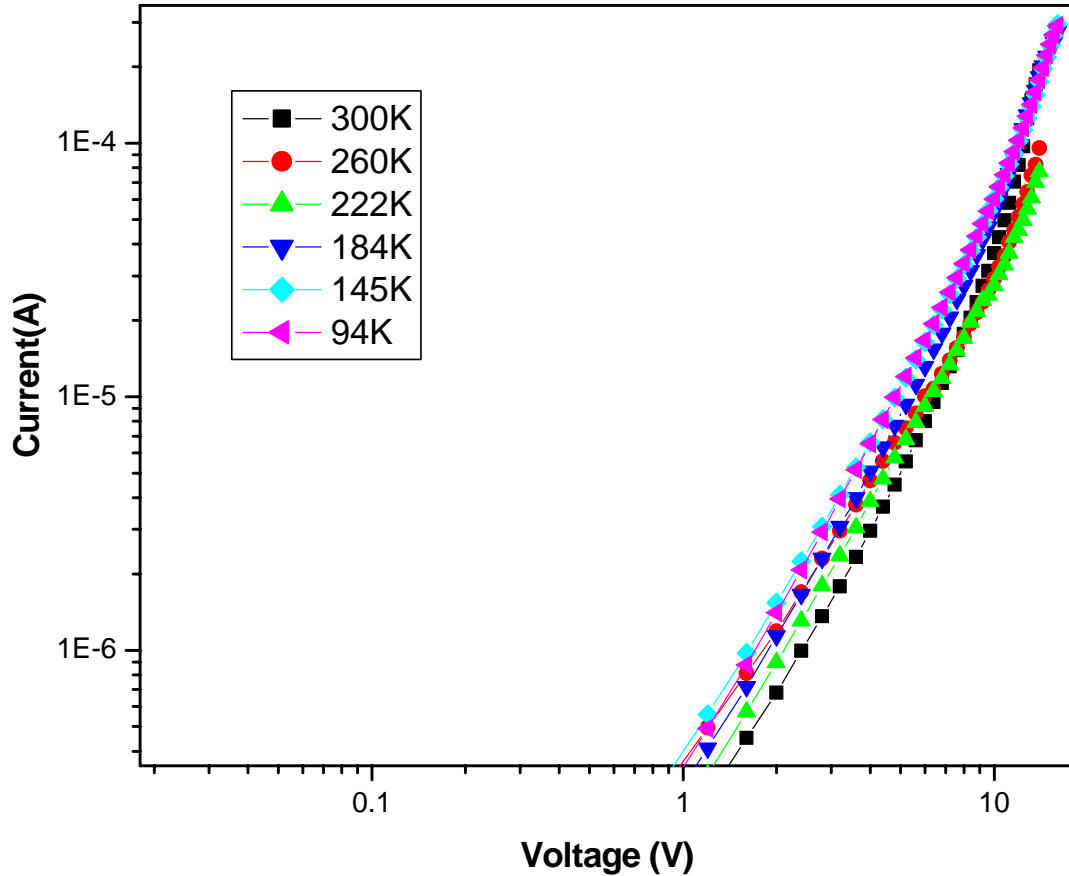


Figure 4.15: Current-Voltage characteristics of the Zn(mq)₂ device showing temperature independent behaviour

The Fowler-Nordheim plot, $\ln(J/F^2)$ vs $1/F$ is shown in **Figure 4.16**. The plot is very close to linear at high field, indicating tunnelling [52]. The deviation from linearity at high voltage is due to the series resistance of the device and degradation of the device arising from Joule heating and that at lower field was thought to be due to a thermionic emission contribution to the current [52, 53]. The barrier height can be obtained from the FN formula [54] using Eqs. (1) and (3). The barrier height is calculated to be 0.01 eV.

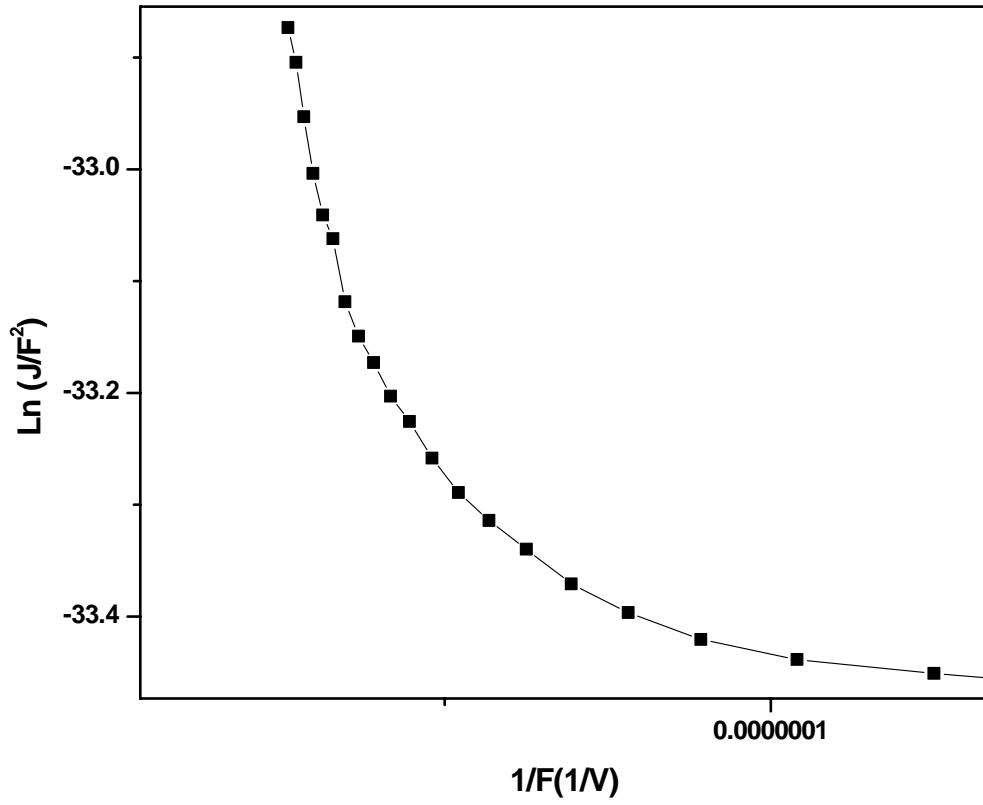


Figure 4.16: The Fowler-Nordheim plot, $\ln(I/F^2)$ vs $1/F$, of $Zn(mq)_2$ device

CHAPTER - 5

CONCLUSION AND FUTURE SCOPE

5.1 Conclusions

The important conclusions of the present study have been summarized as follows:

Znq₂ and Zn(mq)₂ as the novel electroluminescence materials for OLED applications have been synthesized. The materials were structurally characterized by FTIR, TGA and optically characterised by UV-Visible absorption spectra, Photoluminescence spectra. The Photoluminescence properties of thin films of Znq₂ shows maximum absorption at 380 nm, extinction coefficient $7.788 \times 10^3 \text{ moles}^{-1}\text{LCm}^{-1}$, Photoluminescence peak at 542 nm and a quantum yield of 41 % and that of Zn(mq)₂ shows maximum absorption at 385 nm, extinction coefficient of $1.869 \times 10^3 \text{ moles}^{-1}\text{LCm}^{-1}$, Photoluminescence peak at 530 nm and a quantum yield of 21 %. The decomposition temperature was observed at 350 °C for Znq₂ and at 330 °C for Zn(mq)₂. Organic light emitting diode have been fabricated with the structure ITO/ α NPD(40 nm)/Znq₂orZn(mq)₂(35 nm)/BCP(6 nm)/Alq₃(30 nm)/LiF(1 nm)/Al(100 nm), which shows a broad electroluminescence peak at 558 nm when Znq₂ was used as an emissive material and 539 nm when Zn(mq)₂ was used as an emissive material. The I-V characteristics of the device (Znq₂ as an emissive material) shows turn on voltage of about 10.5 V and a maximum brightness 623 cd/m² at 18 V. Whereas for Zn(mq)₂ as an emissive material turn on voltage was of 4.5 V and a maximum brightness 752 cd/m² at 18 V. The maximum brightness of OLED device for Zn(mq)₂ has been found to increase as compared to the OLED device for Znq₂. Also the turn on voltage Zn(mq)₂ device is less compared to Znq₂. But the quantum yield of Zn(mq)₂ is sufficiently less as compared to Znq₂.

Hole only devices of both the Zinc metal complexes (Znq₂ and Zn(mq)₂) have been fabricated. The injection limited current behavior has observed for both the complexes. I-V characteristic of both the devices shows a temperature independent behaviour. Flower Nordiem model fits for both and giving the injection barrier height as 0.025 eV and 0.01 eV for Znq₂ and Zn(mq)₂ device respectively.

5.2 Future Scope

The studies presented in thesis further suggest that there are areas of academic and technological interest. These areas require further investigation. Some of the areas are mentioned as follows

1. A comparative study of Znq_2 and $Zn(mq)_2$ has been done. The effect of attachment of methyl group to the some other metal complexes (Al, Be, B etc. and other rarer earth elements) could be tried for optimizing quantum efficiency, brightness and operating voltage.
2. Temperature dependent Photoluminescence could also be carried out in order to get information about the variation of traps, excitonic vibrations etc.
3. Transport studies could be performed deeply for getting the information about the conduction mechanism i.e. space charge limited current and injection limited current, since it will pave the way for better device fabrication.

REFERENCES:

- [1] J. Kovac, L. Peternai, O. Lengyel, *Thin Solid Films* 22 (2003) 433.
- [2] F. A. Kish et. al. *Appl. Phys. Lett.* 2839 (1994) 64.
- [3] L. Peternai, J. Kovac, G. Irmer, S. Hasenohrl, R. Srnanek, *Microelectronics J.* 487 (2006) 37.
- [4] L. Peternai, J. Kovac, J. Jakabovic, V. Gottschalch, B. Rheinlaender: *J. Electronic Mat.* 654 (2006) 35.
- [5] G. G. Malliaras and R.H. Friend, *Physics Today* 53 (2005) 58.
- [6] C. W. Tang, S.A. Van Slyke, *Appl. Phys. Lett.* 51 (1987) 913.
- [7] Yuji Hamada, *IEEE transactions on electron devices* 44 (1997) 1208.
- [8] C.W. Tang, S.A. Van Slyke, C.H. Chen, *J. Appl. Phys.* 65 (1989) 3611.
- [9] Y. Hamada., T. Sano, M. Fujita, T. Fujii, Y. Nishio, K. Shibata, *Jpn. J. Appl. Phys.* 324A (1993) 514.
- [10] Luminescent Zinc and Lanthanide Complexes Based on 2,2'-Dipyridylamine Derivatives, Wen Yu Yang, Department of Chemistry Queen's University Kingston, Ontario, Canada (August 2000) 22-30.
- [11] V. K. Rai, R. Srivastava, G. Chauhan , K. Saxena, S. Chand, and M.N. Kamalasanan, *Jap.J Appl. Phys.* 47 (2008) (Article in press).
- [12] V. K. Rai, R. Srivastava, G. Chauhan , K. Saxena, R.K. Bharadwaj, S. Chand, and M. N. Kamalasanan, *Mater. Lett.* 2008 (Article in press).
- [13] Y. Hamada , T. Sano, H. Fujii, Y. Nishio, H Takahashi, K. Shibata, *Jpn J. Appl. Phys.* 35Part2 (1996) 1339.
- [14] J. Kido, K. Hongawa, K. Okuyama, K. Nagai, *Appl. Phys. Lett.* 64 (1994) 815.
- [15] S. F. Liu, Q. Wu, H. L. Schmider, H. Aziz, N.X Hu, Z. Popovic, S. Wang, *J Am. Chem. Soc.* 122 (2000) 3671.
- [16] Q. Wu, J. A. Lavigne, S. Wang, *Inorg. Chem.* 39 (2000) 5248.
- [17] Y. K. Jang, D. E. Kim, O. K. Kwon, Y.S Kwon, *Journal of the Korean Physical Society* 49 (2006) 1057.
- [18] N. Donze, P. Pechy, M. Gratzel, M. Schaer, L. Zuppiroli, *Chem Phys. Lett.* 315 (1999) 405.
- [19] A.N. Du, Q. Me, M. Lu, *Synth. Metals* 149 (2005) 193.
- [20] <http://science.howstuffworks.com/oled.htm>.

- [21] <http://en.wikipedia.org/wiki/oled>.
- [22] Organic Light Emitting Diodes (OLEDs) for General Illumination Update 2002
Published by: Optoelectronics Industry Development Association
(<http://www.oida.org>).
- [23] Universal Display Corporation (website).
- [24] L. M. Leung, C. F. Kwong, C. C. Kwok and S.K. So, IEEE, (1999) 18.
- [25] Electroluminescence of conjugated aromatic polymers in organic light emitting diodes Robert h. Lambeth (iii) February 14, 2004.
- [26] Y. Shao, Y. Qiu, W.Hu, Xiaoyin Hong Adv. Mater. Opt. Electron. 10 (2000) 285.
- [27] T. Sano, Y. Nishio, Y. Hamada, H. Takahashi, T. Usuki and K. Shibata, J. Mater. Chem. 10 (2000) 157.
- [28] D. Braun, Journal of Polymer Science: Part B: Polymer Physics 41 (2003) 2622.
- [29] A. Yeh, S. Cherng, Journal of American Science 3 (2007) 4.
- [30] M. A. Lampert, P. Mark, Current Injection in Solids, Academic: New York, 1970.
- [31] P. Mark, W. Helfrich, J Appl Phys 33 (1962) 205.
- [32] T. Mori et al. Applied Surface Science 212–213 (2003) 458–463.
- [33] R. D. Young, Physical Review 113 (1959) 1.
- [34] S. Barth, U. Wolf, and H. Bassler, Physical Review B 60 (1999) 12.
- [35] Y. Sato, S. Ichinosawa, and H. Kanai, IEEE journal of selected topics in quantum electronics 4 (1998) 1.
- [36] S. E. Shaheen, G. E. Jabbour, B. Kippelen, and N. Peyghambarian Applied Physics Letters 74 (1999) 21.
- [37] Y. Shao, Y. Qiu, W. Hu, X. Hong, Adv. Mater. Opt. Electron. 10 (2000) 288.
- [38] T. Sano, Y. Nishio, Y. Hamada, H. Takahashi, T. Usuki and K. Sibata, J. Mater. Chem. 10 (2000) 157.
- [39] Z. D. Popovic and H. Aziz IEEE Journal on Selected Topics in Quantum Electronics 8 (2002) 2.
- [40] I. M. Chan and F. C. Hong, Thin Solid Films 450 (2004) 304.
- [41] N. N. Dinh, D. V. Thanh, P. D. Long, T. Q. Trung International Workshop on Photonics and Applications, Hanoi Vietnam, April 5-8, 2004.
- [42] J. Xie, J. Qiao, L. Wang, J. Xie and Y. Qiu, Inorganica Chimica Acta, 358 (2005) 4451.

- [43] K. W. Sam, Y. J. Min, L. B. Jong, J. Y. Ki, K. D. Eun, K. Y. Soo, *Journal of Nanoscience and Nanotechnology*, 6 (2006) 3637.
- [44] C. Williams et.al *Applied Physics Letters* 88 (2006) 183104.
- [45] V.K. Shukla , S. Kumar and D. Deva, *Journal of Luminescence*, 121 (2006) 132.
- [46] T. Yu, W. Su, W. Li, Z. Hong, R. Hua and B. L. Thin, *Solid Films* 515 (2007) 4080.
- [47] The Royal Society of Chemistry Fine Chemicals and Medicinals Group.
- [48] [http://www.cem.msu.edu/~reusch/VirtualText/Spectrpy/UV- Vis/uvspec.htm](http://www.cem.msu.edu/~reusch/VirtualText/Spectrpy/UV-Vis/uvspec.htm).
- [49] *Organic Spectroscopy* by Willium Kemp.
- [50] <http://science.howstuffworks.com/oled.htm>.
- [51] <http://www.impactanalytical.com/tga.html>.
- [52] I. D. Parker, *J. Appl. Phys.* 75 (1994) 1656.
- [53] P. S. Davids, Sh. M. Kogan, I. D. Parker and D. L. Smith, *Appl. Phys. Lett.* 69 (1996) 2270.
- [54] C. H. Lee, J. Y. Park, Y. W. Park, Y. H. Ahn, D. S. Kim, D. H. Hwang and T. Zyung, *J. Korean Phys. Soc.* 35 (1999) 291.